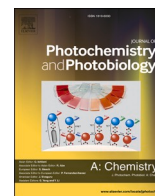




Contents lists available at ScienceDirect

Journal of Photochemistry & Photobiology, A: Chemistry

journal homepage: www.elsevier.com/locate/jphotochemSchiff bases-titanium^(III) & (IV) complex compounds: Novel photocatalysts in Buchwald-Hartwig C–N cross-coupling reactionYahya Absalan^{a,*}, Nazanin Noroozi Shad^a, Mostafa Gholizadeh^{a,*}, Ghodrat Mahmoudi^b, Hossein Sabet Sarvestani^a, Pavel Strashnov^c, Khashayar Ghandi^d, Olga Kovalchukova^c^a Department of Chemistry, Faculty of Science, Ferdowsi University of Mashhad, Mashhad, Iran^b Department of Chemistry, Faculty of Science, University of Maragheh, P.O. Box 55136-553, Maragheh, Iran^c Department of General Chemistry, RUDN University, 6, Miklukha-Maklaya St, Moscow, 117198, Russian Federation^d Department of Chemistry, University of Guelph, 50 Stone Road East Guelph, Ontario, N1G 2W1, Canada

ARTICLE INFO

Keywords:

Complex compounds
Buchwald-Hartwig reaction
Visible-light photocatalyst
Titanium bromide (IV)
Titanium chloride (III)

ABSTRACT

Nine novel Schiff bases were derived from salicylic aldehyde and oxalic aldehyde, isolated, and their molecular and spatial structure were explored by a set of experiments (IR, CNMR, HNMR, CHN, SEM, XRD) and theoretical simulation (DFT def2-TZVP). A high potential was predicted in metal cations chelating. The isolated organic species were applied as the ligands in the reaction of complex formation with titanium (III) chloride and (IV) bromide and 12 novel complexes were synthesized and studied experimentally and theoretically. Using the UV–vis spectroscopic titration, the solution stability of the complexes was indicated. Depending on the nature of the Schiff base ligand, their formation constants were calculated in the range of 6.84–17.32. Using the DFT def2-TZVP theoretical method together with the experimental spectroscopic data, the coordination types of the ligands were investigated, and the structure of the complexes was proposed. The photocatalytic ability of the isolated complexes was tested in the C–N cross-coupling reaction under sunlight. Complexes exhibited high visible-light photocatalytic activity for a wide range of aromatic and benzylic amines including electron-withdrawing and electron-donating groups from moderate to good yields ranging in 50–85 %. The use of an inexpensive, clean, and renewable energy source (visible light) is the superiority of the developed photocatalytic systems.

1. Introduction

The Buchwald–Hartwig amination is a famous organic reaction in carbon-nitrogen coupling through the use of palladium, as the main and usual catalyst, to couple amines with aryl halides [1–4]. This well-known reaction forms a bond between carbon and nitrogen and is highly useful in the synthesis of arylamines for both industrial and research purposes [5].

Numerous reactions are challenged by serious limitations such as functional group tolerance and substrate area. Thanks to the Buchwald-Hartwig reaction, various generations of catalyst complex have been presented, each allowing premier area in connecting associations and gentle reaction situation, offering all amines the possibility of figurative connection with various types of aryl-connecting agents.

Aryl carbon-nitrogen bonds can be found in natural compounds, affecting the entire synthesis of natural compounds and providing a

proper substrate for the preparation of several pharmaceuticals at industrial scales [6–14]. Catalyzed amination of different halides and pseudo-halides has been enhanced and quickly inserted with a suitable ratio to obtain new materials, heterocyclic systems, and pharmaceuticals. It has been recognized as a useful tool for the synthesis of biological compounds [6,15–20].

Such an incredible usage of this method can be assigned to the domination of aromatic amines, which can serve as precursor substances and their importance in biologically active materials [21] (i.e. highly important and vital groups such as kinase inhibitors [22,23], antibiotics [24] and CNS active agents [25]).

In the process of ligands isolation, a similar approach was selected in Schiff bases isolation. The reactants were used to isolate a variety of the potential ligands with different steric properties of the organic species. The changes in the oxidation state of the metal cation (Ti⁺³ or Ti⁺⁴) can lead to different types of electronic and magnetic properties in the

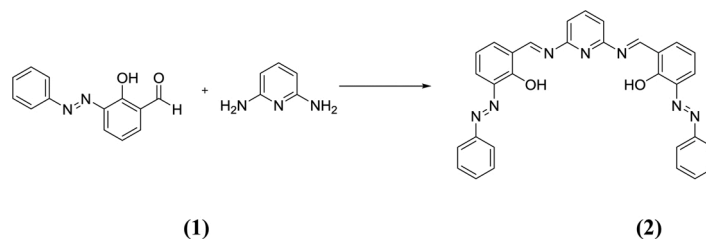
* Corresponding authors.

E-mail addresses: Yahyaabsalan2014@gmail.com (Y. Absalan), m_gholizadeh@um.ac.ir (M. Gholizadeh).<https://doi.org/10.1016/j.jphotochem.2021.113346>

Received 22 February 2021; Received in revised form 10 April 2021; Accepted 5 May 2021

Available online 11 May 2021

1010-6030/© 2021 Elsevier B.V. All rights reserved.



isolated metal complexes. The formation of coordination spheres and multifunctionality of the ligands may result in the formation of coordination polymers with high activities in different catalytic processes. This reflects the key role of the ligands in this type of reaction their influence on the reaction speed and even temperature. Different types of ligands have been employed in this reaction among which, BINAP [26–29], dpfp [30–34], and Xantphos [35–39] can be mentioned. Electron donation plays a key role in this reaction in the favor of the ligand to place phosphines in the first position; Josiphos [40–45], N-heterocyclic carbenes [46–51], and trialkyl phosphines [52–55] are some remarkable instances of electron donation which can increase the substrate area [9, 56].

Although many systems, with the mentioned characters, can be used as catalyzed C-N coupling agents just a limited number of groups work properly. This is directly effective on the feasibility of the catalytic system, its forcefulness, accessibility of substrate, and ligand range [57].

Numerous studies [12,58,67–70,59–66] have addressed other types of ligands to find a suitable condition for an efficient catalyst to be used in a broad range of reactions. Palladium-catalyzed amination Suzuki cross-coupling reaction [71–75], etherification of aryl halides [76], and arylation of enolates [77–81] are some of the well-known instances.

Although the Buchwald-Hartwig reaction was developed to include a group of coupling associations, the situation required for any particular reactants is yet substrate-dependent.

Here, a novel photo-catalyst was derived through new Schiff base ligands and titanium salts (III, IV), as central ions, under visible radiation at room temperature to be applied in the Buchwald-Hartwig amination reaction. By offering donor bonds with titanium metal, ligands changed the energy bandgap toward the visible range. The reaction was carried out between bromobenzene and aromatic amines. The novelties of this research include the synthesis of new groups of Schiff bases, usage of titanium salt (as a cheap and non-poisoning metal) for the first time, and presenting an eco-friendly condition using inexpensive, clean, and renewable visible light as an energy source with proper photocatalytic activity, short reaction time, and excellent yield.

2. Experiment

2.1. Materials and characterization

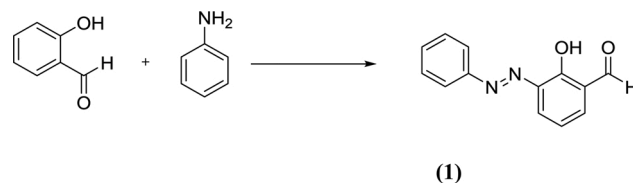
All the precursors, including organic precursors, solvents, and salt metals were purchased from Sigma-Aldrich ($\geq 98\%$) and used as received without further purification. The purity determinations of the products and the progress of the reactions were accomplished by TLC on silica gel Polygram STL G/UV 254 plates. The melting points of the products were determined with an Electrothermal Type 9100 melting point apparatus. X-ray powder diffraction (XRD) was performed using a PANalytical Company X'Pert Pro MPD diffractometer with Cu K α radiation ($\lambda = 0.154$ nm) radiation. FE-SEM images were obtained from a TESCAN, Model: MIRA3 scanning electron microscope operating at an acceleration voltage of 30.0 kV (manufactured by the Czech Republic). The electronic structure calculations were carried out with the ORCA program package ver. 4.1.1. Geometry optimizations were performed using composite approach B97-3c, while wB97 M density functional

method with the Grimme D3 dispersion correction with the Becke-Johnson damping scheme (D3BJ) was employed for single-point calculations [82]. The Ahlrichs' def2-TZVP basis set [83] was used. To study the effect of titanium salts on the ligand in an aqueous environment, UV-vis spectroscopy in the range of 200–800 nm was used by a Cary-50 scan spectrophotometer (Varian). FT-IR spectra were recorded on pressed KBr pellets using an AVATAR 370 FT-IR spectrometer (Thermo Nicolet spectrometer, USA) at room temperature in the wavenumber range of 4000–400 cm^{-1} at a resolution of 4 cm^{-1} . NMR spectra were taken using an NMR Bruker Avance spectrometer at 300 and 400 MHz in CDCl_3 or DMSO. Mass spectra were recorded with a CH7A Varianmat Bremem instrument at 70 eV electron impact ionization, in m/z (rel %). CHN elemental analyses were performed by elemental Thermo Finnigan Flash EA microanalyses whose results were in good agreement ($\pm 0.3\%$) with the calculated values. All yields refer to the isolated products after purification by column chromatography. The photocatalytic coupling experiments were conducted in a capped-sealed test tube.

2.2. Synthesis of Ligand

2.2.1. 6,6'-((1E,1'E)-(pyridine-2,6-diylbis(azanelylidene))bis(methanelylidene))bis(2-((E)-phenyldiazenyl)phenol) (L^1)

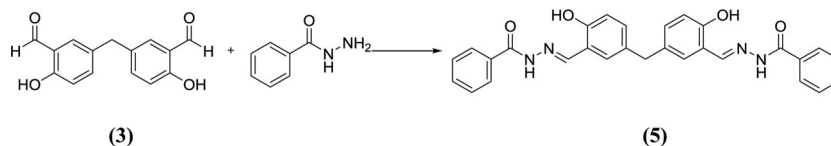
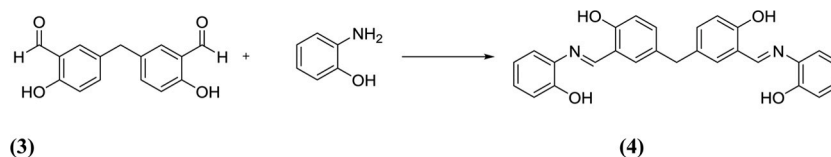
2-hydroxy-3-(phenyldiazenyl)benzaldehyde as an Azo-linked starting material for the synthesis of L^1 is synthesized by the reaction of aniline and salicylaldehyde (1). To a water (20 mL) solution of aniline (0.93 g, 10 mmol) hydrochloric acid (2.5 ml) was added and heated to 70 °C. The mixture was diazotized with dropwise adding sodium nitrite (0.97 g, 14 mmol) dissolved in water (5 mL) between 0 °C–5 °C. Then a solution of salicylaldehyde (1.06 mL, 10 mmol) in water (19 mL) containing NaOH (3.99 g, 10 mmol) was added very slowly in 1 h at 0 °C. The mixture was vigorously stirred for 30 min. The brown solid product was collected by filtration and washed with ethanol and dried under vacuum at 80 °C overnight. Finally the pure product was recrystallized from ethanol.



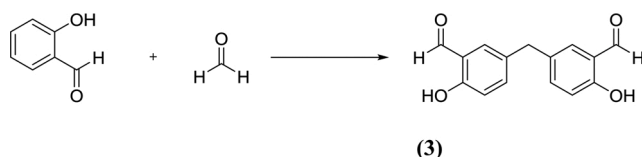
Then, a mixture of 2-hydroxy-3-(phenyldiazenyl)benzaldehyde (2.26 g, 10 mmol) and 2,6-diaminopyridine (0.54 g, 5 mmol) was dissolved in ethanol (20 mL). The solution was refluxed for 2 h. Then it was cooled at room temperature and filtered the mixture. A red solid product has been obtained in the pure form (2). Further purification was gained by recrystallization from ethanol. M.p.: 263 °C; FT-IR (KBr disk): ν 3339, 3058, 1711, 1608, 1595, 1481, 1446, 1405, 1352 cm^{-1} . MS m/z : 525.19 (M^+). Anal. Calcd. For $\text{C}_{31}\text{H}_{23}\text{N}_7\text{O}_2$: C, 70.84; H, 4.41; N, 18.66; Found: C, 68.22; H, 4.15; N, 17.5 %.

2.2.2. 5,5'-Methylenebis(2-hydroxybenzaldehyde)

It is used as a common starting material for the synthesis of L^2 , L^3



ligands. 5,5'-Methylenebis(2-hydroxybenzaldehyde) is synthesized by the reaction of salicylaldehyde (12.2 g, 100 mmol) and formaldehyde (1.5 g, 50 mmol) in glacial acetic acid (20 mL) at room temperature. Then concentrated sulfuric acid (1.0 mL, catalytic) was slowly added to the suspension and the reaction mixture was then allowed to stir at 90 °C for 4 h. After completion of the reaction it was poured on iced water to form the solid product that was collected by filtration and washed with water and hexane. The crude product was obtained as an off-white solid (3).

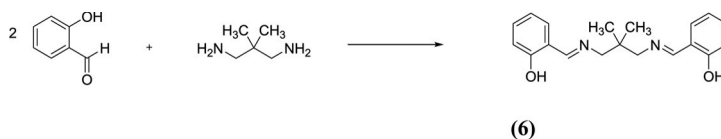


2.2.3. 4,4'-methylenebis(2-((E)-((2-hydroxyphenyl)imino)methyl)phenol) (L^2)

A mixture of 5,5'-Methylenebis(2-hydroxybenzaldehyde) (2.05 g, 8 mmol) and o-aminophenol (1.75 g, 16 mmol) was dissolved in ethanol (20 mL). The solution was refluxed for 60 min. Then it has been cooled at room temperature and filtered the mixture. An orange solid product has been obtained in the pure form (4). Further purification was gained by recrystallization from ethanol. M.p.: 226 °C; ^1H NMR (300 MHz, DMSO): δ 3.91 (s, 2H, CH_2), 6.85–7.48 (m, 14H, Ar), 8.94 (s, 2H, C = N), 9.72 (s, 2H, OH, D_2O exchangeable), 13.62 (s, 2H, OH, D_2O exchangeable); ^{13}C NMR (75 MHz, DMSO): δ 116.9, 117.2, 119.7, 120, 128.4, 132, 132.3, 133.8, 135.4, 151.5, 159.5, 161.9; FT-IR (KBr disk): ν 3043, 2896, 2831, 1636, 1592, 1490, 1459, 1275, 1137 cm^{-1} ; MS m/z : 438 (M^+). Anal. Calcd. For $\text{C}_{27}\text{H}_{22}\text{N}_2\text{O}_4$: C, 73.96; H, 5.06; N, 6.39; Found: C, 72.47; H, 4.79; N, 5.39 %.

2.2.4. N',N'' -((1E,1'E)-(methylenebis(6-hydroxy-3,1-phenylene))bis(methaneylylidene)) di(benzohydrazide) (L^3)

To a stirring solution of benzhydrazide (2.17 g, 16 mmol) in ethanol (15 mL), 5,5'-methylene-bis-salicylaldehyde (2.05 g, 8 mmol) was added. The mixture then refluxed for 4 h. The white solid was filtered-off and washed with ethanol and dried over CaCl_2 (5). The crude product was purified by recrystallization from ethanol.



2.2.5. 2,2'-((1E,1'E)-((2,2-dimethylpropane-1,3-diyl)bis(azaneylylidene)) bis(methaneylylidene)) diphenol (L^4)

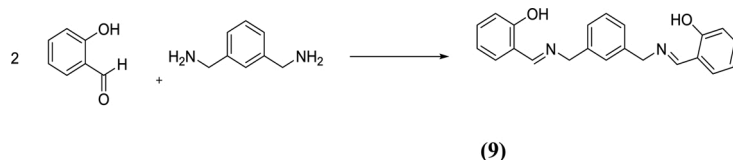
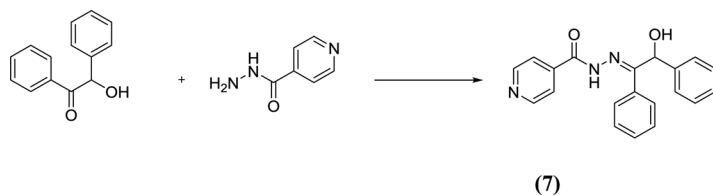
For the synthesis of Schiff base ligand (L^4), the methanolic solution (10 mL) of 2,2-Dimethyl-1,3-diaminopropane (0.10 g, 1 mmol) was added to the methanolic solution (10 mL) of 2-hydroxybenzaldehyde (0.24 g, 2 mmol). After stirring (30 min) of the resulting solution at room temperature, a yellow sediment was obtained and separated by vacuum filtration, washed with methanol and dried in a desiccator (6). M.p.: 86 °C; ^1H NMR (300 MHz, DMSO): δ 1.12 (t, $J = 6$, 6H, CH_3), 3.53 (s, 4H, CH_2), 6.90–7.39 (m, 8H, Ar), 8.38 (s, 2H, C = N), 13.60 (s, 2H, OH, D_2O exchangeable); ^{13}C NMR (75 MHz, DMSO): δ 24.41, 36.2, 68.1, 116.9, 118.6, 118.7, 131.3, 132.3, 161.2, 165.7; FT-IR (KBr disk): ν 3064, 3005, 2962, 2881, 2831, 2725, 1631, 1580, 1497, 1275 cm^{-1} ; MS m/z : 310 (M^+). Anal. Calcd. For $\text{C}_{19}\text{H}_{22}\text{N}_2\text{O}_2$: C, 73.52; H, 7.14; N, 9.03; Found: C, 71.2; H, 6.95; N, 9.26 %.

2.2.6. (Z)-N'-(2-hydroxy-1,2-diphenylethylidene)isonicotinohydrazide (L^5)

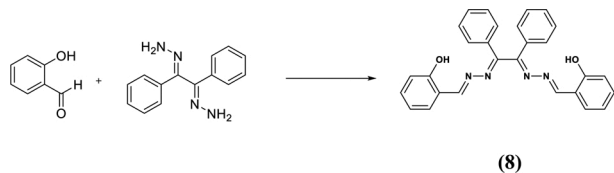
To a stirring solution of 2-Hydroxy-2-phenylacetophenone (2.12 g, 10 mmol) in ethanol (20 mL), 4-pyridinecarboxylic acid hydrazide (1.37 g, 10 mmol) was added. Then glacial acetic acid (0.1 mL, as a catalyst) was slowly added to the reaction mixture was then allowed to stir at 75 °C for 5 h. Then it has been cooled at room temperature and filtered the solid product in the pure form (7). M.p.: 111 °C; ^1H NMR (300 MHz, DMSO) δ 10.15 (s, 1 H), 8.86 (s, 1 H), 8.73 (d, $J = 5.1$ Hz, 2 H), 8.03 (d, $J = 7.7$ Hz, 2 H), 7.77 (d, $J = 5.1$ Hz, 2 H), 7.58 (t, $J = 7.3$ Hz, 1 H), 7.46 (q, $J = 7.4$ Hz, 4 H), 7.33 (t, $J = 7.4$ Hz, 2 H), 7.25 (t, $J = 7.2$ Hz, 1 H), 6.11 (q, $J = 6.3$, 5.6 Hz, 2 H), 4.73 (s, 2 H), 4.54 (s, 1 H). ^{13}C NMR (75 MHz, DMSO) δ 199.68, 164.41, 150.69, 140.76, 140.23, 135.21, 133.71, 129.33, 129.07, 128.96, 128.19, 127.78, 126.92, 121.50, 76.17. FT-IR (KBr disk): ν 3413, 3059, 2933, 1676, 1596, 1458, 1263 cm^{-1} ; MS m/z : 333 (M^+). Anal. Calcd. For $\text{C}_{20}\text{H}_{19}\text{N}_3\text{O}_2$: C, 72.49; H, 5.17; N, 12.68; Found: C, 72.20; H, 5.62; N, 12.51 %.

2.2.7. 2,2'-((1E,1'E)-(((1E,2E)-1,2-diphenylethane-1,2-diylidene)bis(hydrazine-2,1-diylidene)) bis(methaneylylidene)) diphenol (L^6)

To a stirring solution of salicylaldehyde (2.44 g, 20 mmol) in ethanol (20 mL), Benzyl Dihydrazone (2.38 g, 10 mmol) was added. Then glacial acetic acid (0.1 mL, as a catalyst) was slowly added to the reaction mixture was then allowed to stir at 75 °C for 6 h. Then it has been



cooled at room temperature and filtered the solid product in the pure form (**8**). M.p.: 193 °C; ^1H NMR (300 MHz, DMSO) δ 10.90 (s, 1 H), 9.03 (s, 1 H), 7.94 – 7.82 (m, 2 H), 7.61 – 7.45 (m, 4 H), 7.32 (ddd, $J = 8.7, 7.4, 1.7$ Hz, 1 H), 6.94 – 6.79 (m, 2 H). ^{13}C NMR (76 MHz, DMSO) δ 165.79, 164.86, 159.24, 134.05, 132.96, 132.47, 132.42, 129.82, 127.86, 120.02, 118.21, 116.95, 76.28; FT-IR (KBr disk): ν 3385, 3050, 2929, 1603, 1466, 1268 cm^{-1} ; MS m/z : 446 (M^+). Anal. Calcd. For $\text{C}_{28}\text{H}_{22}\text{N}_4\text{O}_2$: C, 75.32; H, 4.97; N, 12.55; Found: C, 75.50; H, 4.76; N, 13.39 %.

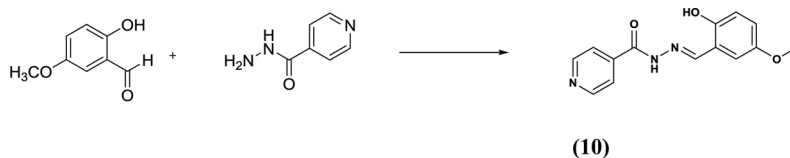


2.2.8. 2,2'-((1E,1'E)-((1,3phenylenebis(methylene))bis(azaneylylidene)) bis(methaneylylidene)) diphenol (**L**⁷)

To a stirring solution of salicylaldehyde (2.44 g, 20 mmol) in ethanol (20 mL), *m*-Xylylenediamine (1.36 g, 10 mmol) was added. Then glacial acetic acid (0.1 mL, as a catalyst) was slowly added to the reaction mixture was then allowed to stir at 75 °C for 6 h. Then it was cooled at room temperature and filtered the solid product in the pure form (**9**). M. p.: 48 °C; ^1H NMR (300 MHz, DMSO) δ 13.45 (s, 1 H), 8.73 (d, $J = 1.3$ Hz, 1 H), 7.49 (dd, $J = 7.6, 1.8$ Hz, 1 H), 7.46 – 7.24 (m, 3 H), 6.99 – 6.86 (m, 2 H), 4.83 (s, 2 H). ^{13}C NMR (75 MHz, DMSO) δ 167.07, 161.01, 139.51, 132.92, 132.25, 129.41, 127.75, 127.18, 119.20, 119.13, 116.95, 62.49. FT-IR (KBr disk): ν 3423, 3025, 2939, 2898, 2845, 1608, 1491, 1284 cm^{-1} ; MS m/z : 344 (M^+). Anal. Calcd. For $\text{C}_{22}\text{H}_{20}\text{N}_2\text{O}_2$: C, 76.72; H, 5.85; N, 8.13; Found: C, 76.65; H, 5.68; N, 8.21 %.

2.2.9. (E)-N'-(2-hydroxy-5-methoxybenzylidene)isonicotinohydrazide (**L**⁸)

To a stirring solution of 2-Hydroxy-5-methoxybenzaldehyde (1.52 g, 10 mmol) in ethanol (20 mL), 4-pyridinecarboxylic acid hydrazide (1.37 g, 10 mmol) was added. Then glacial acetic acid (0.1 mL, as a



catalyst) was slowly added to the reaction mixture was then allowed to stir at 75 °C for 5 h. Then it has been cooled at room temperature and filtered the solid product in the pure form (**10**). M.p.: 198 °C; ^1H NMR (300 MHz, DMSO) δ 12.33 (s, 1 H), 10.62 (s, 1 H), 8.85 – 8.74 (m, 2 H), 8.71 (s, 1 H), 7.92 – 7.84 (m, 2 H), 7.18 (d, $J = 2.6$ Hz, 1 H), 7.01 – 6.80 (m, 2 H), 3.73 (d, $J = 1.0$ Hz, 3 H). ^{13}C NMR (75 MHz, DMSO) δ 161.89, 152.65, 152.12, 150.77, 150.04, 149.03, 140.47, 123.32, 122.00, 119.35, 119.08, 117.82, 112.48, 55.88. FT-IR (KBr disk): ν 3433, 3200, 3065, 2954, 2839, 1653, 1583, 1494, 1272 cm^{-1} ; MS m/z : 271 (M^+). Anal. Calcd. For $\text{C}_{14}\text{H}_{13}\text{N}_3\text{O}_3$: C, 61.99; H, 4.83; N, 15.49; Found: C, 62.11; H, 4.91; N, 15.36 %.

2.2.10. 2,2'-(((1E,2E)-ethane-1,2-diylidene)bis(azaneylylidene)) diphenols (**L**⁹)

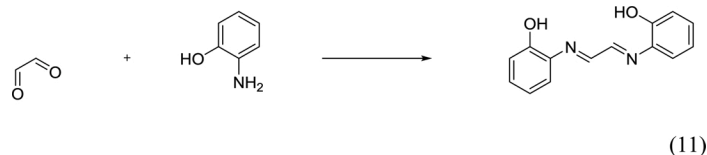
To a stirring solution of Oxalaldehyde (1.14 mL, 10 mmol) in ethanol (20 mL), 2-Aminophenol (2.18 g, 20 mmol) was added. Then glacial acetic acid (0.1 mL, as a catalyst) was slowly added to the reaction mixture was then allowed to stir at 75 °C for 5 h. Then it has been cooled at room temperature and filtered the solid product in the pure form (**11**). M.p.: 223 °C; ^1H NMR (300 MHz, DMSO) δ 7.34 (d, $J = 4.2$ Hz, 1 H), 6.71 (dtd, $J = 21.5, 14.7, 7.7$ Hz, 5 H), 6.54 (s, 2 H), 5.30 (d, $J = 4.1$ Hz, 1 H). ^{13}C NMR (75 MHz, DMSO) δ 141.77, 130.63, 121.86, 119.13, 116.55, 114.67, 75.77. FT-IR (KBr disk): ν 3383, 3048, 2934, 1609, 1499, 1257 cm^{-1} ; MS m/z : 240 (M^+). Anal. Calcd. For $\text{C}_{14}\text{H}_{12}\text{N}_2\text{O}_2$: C, 69.99; H, 5.03; N, 11.66; Found: C, 69.82; H, 5.11; N, 11.54 %.

2.3. Synthesis of complexes

2.3.1. General synthesis of complexes

TiCl_3 (M_1) and TiBr_4 (M_2) were used as salt metals to be coordinated by the obtained ligands. Generally, all the complexes were obtained by the following method:

Solvents were different according to the salt metals. Methanol was used for TiCl_3 (Ti^{III}), as the solvent, and acetone was used for TiBr_4 (Ti^{IV}) complexes. The corresponding ligand was dissolved in the chosen solvent (2×10^{-3}) and mixed for 30 min, and salt metal was also dissolved (2×10^{-4}) in the same solvent, then it was added drop by drop to the solution of ligand and it was stirred for 12 h under argon environment.



There is just a difference between L^1 , L^2 , and L^3 with other ligands, and it was usage of NaOH for solving these ligands. Other ligands were dissolved just to the solvent.

After precipitate was appeared, stirring was continued to complete the reaction, then precipitate was separated from solvent and dried in the vacuum autoclave at 30°C for 24 h.

The characterization has been carried out by different methods, which according to each complex and based on the nature of the complexes, it was different.

2.3.2. $Ti^{IV}(L^1)(OH)_2H_2O$, (M_2L^1), (1)

The procedure was the same as the general method. After adding $TiBr_4$ solution to the ligand, which was solved in the same solvent (acetone) and 1 drop NaOH (1 mol), immediately the colour changed from light red to dark red. The precipitate immediately appeared, and to complete the reaction it was kept in the reaction solution for 12 h. 1H NMR (300 MHz, DMSO) δ 12.31 (s, 1 H), 7.91 – 7.75 (m, 3 H), 7.83 (s, 23 H), 7.55 (s, 43 H), 7.51 (s, 3 H), 2.25 – 2.12 (m, 2 H), 2.11 (s, 2 H), 2.10 (s, 18 H), 2.06 (d, $J=3.5$ Hz, 2 H), 2.08 – 1.93 (m, 2 H), 1.85 (d, $J=1.3$ Hz, 2 H), 1.23 (s, 1 H), 1.22 (s, 2 H), 1.16 (s, 2 H). ^{13}C NMR (76 MHz, DMSO) δ 141.74, 130.59, 121.84, 119.98, 119.10, 116.52, 114.65, 75.76, 31.17. FT-IR (KBr disk): ν 3433, 3200, 3065, 2954, 2839, 1653, 1583, 1494, 1272 cm^{-1} ; MS m/z : 271 (M^+). Anal. Calcd. For $C_{14}H_{13}N_3O_3$: C, 61.99; H, 4.83; N, 15.49; Found: C, 62.11; H, 4.91; N, 15.36 %.

2.3.3. $Ti^{III}(L^2)(OH)_2$, (M_1L^2), (2)

The procedure was the same as the general method. After adding $TiCl_3$ solution to the ligand, which was solved in the same solvent (methanol) and 1 drop NaOH (1 mol), immediately the colour changed from orange to red. The precipitate immediately appeared, and to complete the reaction it was kept in the reaction solution for 12 h. 1H NMR (300 MHz, DMSO) δ 8.97 (s, 2 H), 7.48 (d, $J=2.2$ Hz, 2 H), 7.43 (s, 1 H), 7.35 (dd, $J=7.9, 1.6$ Hz, 2 H), 7.29 (d, $J=2.2$ Hz, 1 H), 7.26 (d, $J=2.3$ Hz, 1 H), 7.12 (td, $J=7.6, 7.2, 1.6$ Hz, 2 H), 7.01 (d, $J=8.0$ Hz, 2 H), 6.96 (s, 2 H), 6.94 – 6.77 (m, 5 H), 3.91 (s, 2 H), 3.83 (s, 0 H). ^{13}C NMR (76 MHz, DMSO) δ 161.84, 159.63, 151.89, 135.40, 133.75, 132.28, 132.02, 128.41, 120.16, 119.82, 117.30, 117.11. FT-IR (KBr disk): ν 3060, 2900, 2835, 1614, 1597, 1490, 1469, 1281, 1142 cm^{-1} . MS m/z : 563 (M^+); Anal. Calcd. For $Ti_2C_{27}H_{20}N_2O_6$: C, 57.48; H, 3.57; N, 4.97, Ti, 16.97; Found: C, 56.31; H, 3.93; N, 3.70, Ti, 17.03 %.

2.3.4. $Ti^{IV}(L^2)Br_4$, (M_2L^2), (3)

This complex was prepared in a way similar to that of 1. The colour changed from orange to red. 1H NMR (300 MHz, DMSO) δ 10.58 (d, $J=5.8$ Hz, 1 H), 10.39 (s, 5 H), 10.24 (d, $J=2.6$ Hz, 1 H), 8.12 (d, $J=3.3$ Hz, 2 H), 7.72 (s, 1 H), 7.49 (dt, $J=6.5, 2.3$ Hz, 1 H), 7.41 (ddd, $J=10.7, 4.3, 2.4$ Hz, 2 H), 7.32 – 7.23 (m, 2 H), 7.26 – 7.19 (m, 1 H), 7.17 (ddd, $J=15.7, 8.1, 2.6$ Hz, 1 H), 7.05 (dt, $J=7.8, 1.6$ Hz, 1 H), 7.05 – 6.86 (m, 5 H), 6.86 – 6.65 (m, 3 H), 6.16 (d, $J=1.3$ Hz, 1 H), 3.85 (t, $J=5.0$ Hz, 2 H), 3.19 (s, 1 H), 2.91 (s, 1 H), 2.75 (s, 1 H), 2.50 (s, 1 H), 2.33 (d, $J=10.1$ Hz, 1 H), 2.11 (s, 6 H), 2.25 – 2.03 (m, 5 H), 2.03 – 1.90 (m, 2 H), 1.95 – 1.81 (m, 2 H), 1.43 (s, 1 H), 1.41 (s, 1 H), 1.33 (s, 0 H), 1.25 (s, 5 H), 1.16 (s, 4 H), 0.86 (q, $J=7.2, 6.6$ Hz, 1 H); ^{13}C NMR (76 MHz, DMSO) δ 18.92, 39.92, 39.65, 39.37, 56.55. FT-IR (KBr disk): ν 3064, 2896, 2920, 1612, 1586, 1468, 1282, 1158 cm^{-1} ; MS m/z : 850 (M^+). Anal. Calcd. For $C_{27}H_{18}Br_4N_2O_4Ti_2$: C, 38.16; H, 2.14; N, 3.30, Ti,

11.27, Br, 37.61; Found: C, 33.76; H, 3.62; N, 4.33, Ti, 13.27, Br, 35.32 %

2.3.5. $Ti^{IV}(L^3)Br_4(OH)_2$, (M_2L^3), (4)

This complex was prepared in a way similar to that of 1. The colour changed from pale yellow to red. 1H NMR (300 MHz, DMSO) δ 7.81 (s, 1 H), 6.81 (d, $J=15.1$ Hz, 2 H), 2.30 (s, 2 H), 2.11 (s, 31 H). ^{13}C NMR (76 MHz, DMSO) δ 207.36, 31.14. FT-IR (KBr disk): ν 3200, 3045, 3025, 2017, 2832, 1623, 1645, 1531, 1489, 1349, 1279 cm^{-1} . MS m/z : 906 (M^+). Anal. Calcd. For $C_{29}H_{22}Br_4N_4O_4Ti_2$: C, 38.45; H, 2.45; N, 6.19, Ti, 10.57, Br, 35.28; Found: C, 38.37; H, 2.66; N, 6.15, Ti, 10.54, Br, 34.28 %.

2.3.6. $Ti^{IV}(L^4)Br_2$, (M_2L^4), (5)

This complex was prepared in a way similar to that of 1. However, NaOH was not used to dissolve the ligand in the solvent. The colour changed from green to orange. 1H NMR (300 MHz, DMSO) δ 7.84 (s, 7 H), 7.68 (dd, $J=7.7, 1.8$ Hz, 1 H), 7.54 (ddd, $J=8.4, 7.2, 1.8$ Hz, 2 H), 7.39 (s, 1 H), 7.09 – 6.95 (m, 2 H), 6.97 (s, 2 H), 7.01 – 6.89 (m, 2 H), 3.54 (s, 2 H), 2.84 (d, $J=5.9$ Hz, 2 H), 2.81 (s, 2 H), 2.11 (s, 37 H), 1.09 (d, $J=4.0$ Hz, 2 H), 1.02 (d, $J=3.6$ Hz, 9 H). ^{13}C NMR (76 MHz, DMSO) δ 46.32, 33.20, 31.16, 22.76. FT-IR (KBr disk): ν 2966, 2926, 2806, 2881, 2598, 1656, 1605, 1541, 1261 cm^{-1} ; MS m/z : 516 (M^+). Anal. Calcd. For $C_{19}H_{20}Br_2N_2O_2Ti$: C, 44.22; H, 3.91; N, 5.43, Ti, 9.28, Br, 30.97; Found: C, 44.22; H, 3.01; N, 5.65, Ti, 10.12, Br, 29.73 %.

2.3.7. $Ti^{IV}(L^5)Br_2(OH)$, (M_2L^5), (6)

This complex was prepared in a way similar to that of 5. The colour changed from colourless to pale brown. FT-IR (KBr disk): ν 3395, 2966, 2926, 1656, 1605, 1541, 1261 cm^{-1} ; MS m/z : 555 (M^+). Anal. Calcd. For $C_{20}H_{17}Br_2N_3O_3Ti$: C, 43.28; H, 3.09; N, 7.57, Ti, 8.62, Br, 28.79; Found: C, 47.71; H, 3.30; N, 6.53, Ti, 9.22, Br, 27.63 %.

2.3.8. $Ti^{III}(L^6)Cl_4.9H_2O$, (M_1L^6), (7)

The ligand was dissolved (2×10^{-3}) in a mix of methanol and ethanol with 80 % and 20 %, respectively. Then $TiCl_3$ with the same concentration was added and after 30 min, mixing at the room temperature, the temperature was adjusted to 40°C through the oil bath for 2 h refluxing, the light green colour changed to brown light honey like colour. After completing the reaction, the precipitate was separated from the solvent, and then dried in the vacuum autoclave at 30°C to a constant mass. 1H NMR (300 MHz, DMSO) δ 10.84 (s, 1 H), 9.01 (s, 1 H), 8.11 – 7.91 (m, 1 H), 7.89 – 7.74 (m, 4 H), 7.71 – 7.61 (m, 1 H), 7.66 – 7.55 (m, 1 H), 7.55 (d, $J=4.0$ Hz, 4 H), 7.55 – 7.40 (m, 2 H), 7.43 – 7.19 (m, 10 H), 7.19 – 7.10 (m, 3 H), 7.10 – 6.73 (m, 5 H), 6.66 (t, $J=7.4$ Hz, 1 H), 2.42 (s, 1 H), 2.25 – 1.97 (m, 1 H), 1.75 – 1.28 (m, 2 H), 1.25 (s, 2 H), 1.26 – 1.08 (m, 1 H). ^{13}C NMR (76 MHz, DMSO) δ 164.70, 159.14, 134.07, 132.95, 132.43, 130.67, 130.08, 130.01, 129.84, 128.91, 128.81, 128.04, 127.83, 120.07, 118.23, 116.93. FT-IR (KBr disk): ν 3154, 2921, 1606, 1486, 1272 cm^{-1} . MS m/z : 841 (M^+). Anal. Calcd. For $C_{28}H_{35}Cl_4N_4O_{11}Ti_2$: C, 39.81; H, 4.50; N, 6.63; Ti, 11.38; Cl, 16.86; Found: C, 39.70; H, 4.48; N, 6.66; Ti, 12.22; Cl, 15.71 %.

2.3.9. $Ti^{III}(L^7)OH.4H_2O$, (M_1L^7), (8)

This complex was prepared in a way similar to that of 7. The colour changed from light green to yellow. FT-IR (KBr disk): ν 3391, 3020, 2948, 1592, 1491, 1311 cm^{-1} ; MS m/z : 540 (M^+). Anal. Calcd. For

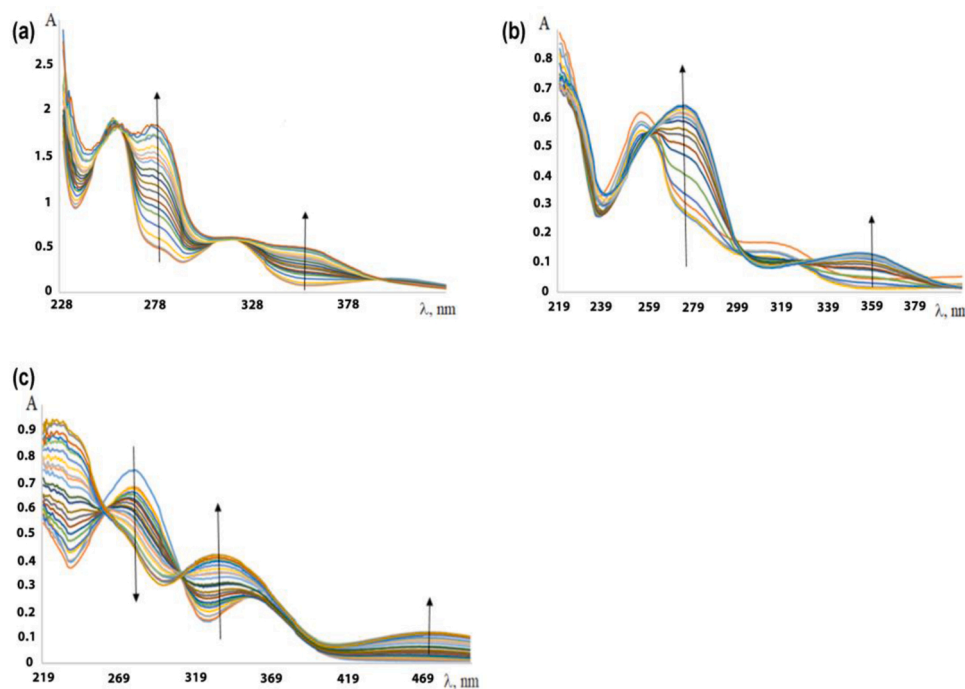


Fig. 1. Change of the UV-vis spectra of ethanol solutions of L^4 (a), L^7 (b), and L^8 (c) at dropwise addition of a solution of $TiCl_3$ (arrow show the change in absorption).

$C_{24}H_{31}N_2O_6Ti_2$: C, 53.36; H, 5.97; N, 5.19; Ti, 17.72; Found: C, 55.03; H, 5.72; N, 5.20; Ti, 16.91 %.

2.3.10. $(Ti^{IV}O)_2(L^7)Br_2$, (M_2L^7), (9)

This complex was prepared in a way similar to that of 1. The colour changed from green to orange. 1H NMR (301 MHz, DMSO) δ 8.32 (s, 5 H), 7.66–7.46 (m, 3 H), 6.88 (s, 3 H), 4.07 (s, 3 H), 2.10 (s, 20 H). ^{13}C NMR (76 MHz, DMSO) δ 139.06, 134.65, 132.32, 130.00, 129.60, 129.34, 127.05, 116.67, 42.58, 27.87. FT-IR (KBr disk): ν 3395, 3023, 2959, 2700, 2602, 1704, 1598, 1500, 1311 cm^{-1} ; MS m/z : 630 (M^+). Anal. Calcd. For $C_{22}H_{18}Br_2N_2O_4Ti_2$: C, 41.95; H, 2.88; N, 4.45; Ti, 15.20; Br, 25.37; Found: C, 42.97; H, 3.28; N, 5.05; Ti, 15.20; Br, 25.37 Ti, 16.18; Br, 14.23 %.

2.3.11. $Ti^{III}(L^8)Cl_2 \cdot H_2O$, (M_1L^8), (10)

This complex was prepared in a way similar to that of 2. The colour changed from pale yellow to red wine. FT-IR (KBr disk): ν 3329, 3054, 2943, 2832, 1642, 1579, 1508, 1270 cm^{-1} ; MS m/z : 408 (M^+). Anal. Calcd. For $C_{14}H_{16}Cl_2N_3O_4Ti$: C, 41.11; H, 3.94; N, 10.27; Ti, 11.70; Cl, 17.33; Found: C, 42.56; H, 3.20; N, 8.89; Ti, 10.35; Cl, 16.98 %.

2.3.12. $(Ti^{IV}O)(L^8)Br$, (M_2L^8), (11)

This complex was prepared in a way similar to that of 1. The colour changed from pale yellow to red. 1H NMR (300 MHz, DMSO) δ 12.45 (s, 1 H), 9.19 (s, 1 H), 9.01–8.91 (m, 1 H), 8.86–8.78 (m, 2 H), 8.13–8.02 (m, 1 H), 8.02–7.94 (m, 2 H), 7.49 (d, $J=3.2$ Hz, 1 H), 7.25–7.15 (m, 1 H), 7.01–6.81 (m, 1 H), 6.75 (d, $J=9.0$ Hz, 1 H), 4.51 (s, 12 H), 3.78 (d, $J=18.7$ Hz, 5 H), 2.10 (s, 1 H). ^{13}C NMR (76 MHz, DMSO) δ 166.15, 161.35, 157.29, 154.25, 153.22, 152.67, 152.00, 149.41, 149.06, 148.82, 147.71, 142.72, 124.88, 124.12, 123.49, 123.08, 119.41, 117.89, 116.93, 112.01, 56.29, 55.99. FT-IR (KBr disk): ν 3380, 3047, 3065, 2835, 2574, 1634, 1589, 1559, 1271 cm^{-1} ; MS m/z : 478 (M^+). Anal. Calcd. For $C_{14}H_{13}BrN_3O_5Ti_2$: C, 35.11; H, 2.74; N, 8.77; Ti, 19.99; Br, 16.68; Found: C, 37.56; H, 3.19; N, 8.89; Ti, 21.03; Br, 15.23 %.

2.3.13. $(Ti^{IV}O)_2(L^9)Br_2$, (M_2L^9), (12)

This complex was prepared in a way similar to that of 2. The colour

changed from orange to dark green. 1H NMR (300 MHz, DMSO) δ 9.93 (s, 2 H), 7.33 (d, $J=4.2$ Hz, 2 H), 7.00 (d, $J=7.6$ Hz, 1 H), 6.88 (d, $J=2.4$ Hz, 2 H), 6.82–6.56 (m, 12 H), 5.27 (d, $J=3.9$ Hz, 3 H), 3.18 (s, 1 H), 2.10 (s, 23 H), 2.17–2.03 (m, 2 H), 1.92–1.83 (m, 1 H), 1.25 (s, 1 H), 1.16 (s, 1 H). ^{13}C NMR (76 MHz, DMSO) δ 199.40, 160.31, 145.64, 138.20, 131.38, 129.88, 128.22, 125.85, 124.84, 124.58, 122.67, 122.05, 117.43, 31.89, 29.83, 28.02. FT-IR (KBr disk): ν 3398, 3048, 3219, 1609, 1495, 1266 cm^{-1} ; MS m/z : 528 (M^+). Anal. Calcd. For $C_{14}Br_2H_{12}N_2O_4Ti_2$: C, 31.86; H, 2.29; N, 5.31; Ti, 18.14; Br, 30.28; Found: C, 32.56; H, 3.19; N, 6.37; Ti, 17.12; Br, 31.23 %.

2.4. Typical procedure for C-N cross coupling reaction

The procedure for the C-N cross coupling reaction was the same for the different heterogeneous photocatalysts. In a typical procedure, to a stirred mixture of bromobenzene (1 mmol, 0.093 g), aniline derivatives (1 mmol) and K_2CO_3 (1 mmol, 0.138 g) in DMF (4 mL), M_1L^8 (10) (0.4 mol%, 0.0016 g) was added. The reaction mixture was located under sunlight irradiation at ambient temperature (a sunny day, in July, in Mashhad between 10 am to 5 pm at the temperature ranges of 22–34 $^{\circ}C$). The reaction was monitored by TLC. The reaction mixture colour changed from yellow to brown. After completion of the reaction, the catalyst was separated and the desired product was extracted by ethyl acetate (4 mL). The obtained crude product was purified by thin layer chromatography using n-hexane/ethyl acetate (50:1).

3. Results and discussion

3.1. Synthesis and characterization

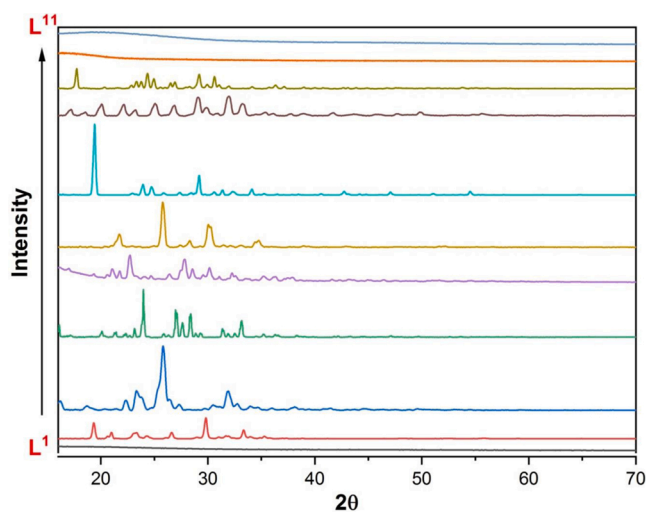
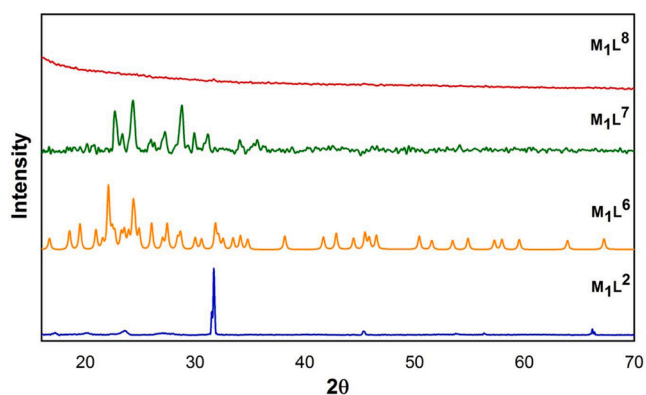
The organic ligands L^1 – L^9 were isolated and purified using general procedures of condensation of aldehydes and ketones with amines and hydrazides. The purity of the basic products was explored by thin layer chromatography. The mass spectra of the compound contain signals corresponding to the molecular ion (M^+). The IR and NMR spectra indicated bands and signals of characteristic fragments and functional groups which will be discussed later.

The ability of L^1 – L^9 to form complexes with Ti^{III} and Ti^{IV} species was

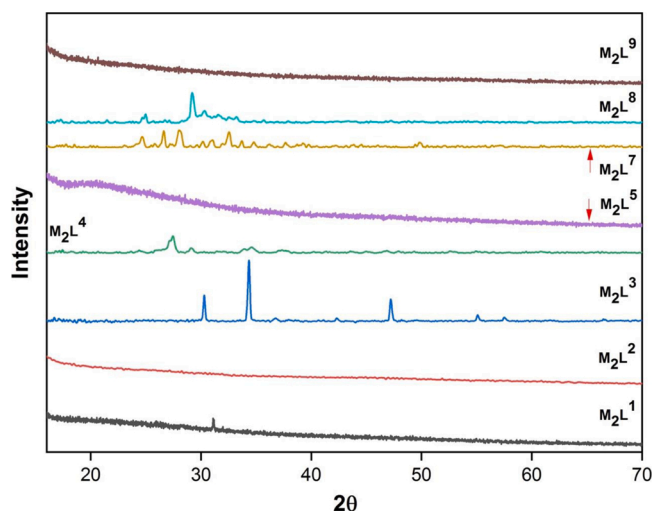
Table 1

Features of the complexes in aqueous solution from analysis of their UV–vis spectra.

Compounds	n (ML _n)	Logβ	Logβ/n	λ _{max}
Ti ^{IV} (L ¹)(OH) ₂ ·H ₂ O	2	19.02	9.51	265
Ti ^{III} ₂ (L ²)(OH) ₂	2	15.38	7.69	341
Ti ^{IV} ₂ (L ²)Br ₄	2	16.20	8.1	361
Ti ^{IV} ₂ (L ³)Br ₄ (OH) ₂	2	18.51	9.25	266
Ti ^{IV} (L ⁴)Br ₂	1	17.32	17.32	405
Ti ^{IV} (L ⁵)Br ₂ (OH)	1	6.84	6.84	266
Ti ^{III} ₂ (L ⁶)Cl ₄ ·9H ₂ O	1	11.43	11.43	303
Ti ^{III} (L ⁷)OH·4H ₂ O	1	10.929	10.929	278
(Ti ^{IV} O) ₂ (L ⁷)Br ₂	1	9.59	9.59	261
Ti ^{III} (L ⁸)Cl ₂ ·H ₂ O	1	7.94	7.94	283
(Ti ^{IV} O)(L ⁸)Br	1	10.048	10.048	272
(Ti ^{IV} O) ₂ (L ⁹)Br ₂	1	8.20	8.20	279

**Fig. 2.** XRD pattern of the ligands.**Fig. 3.** XRD pattern of M₁L^x.

examined by the UV–vis spectroscopic titration method (Fig. 1). In all the cases, a redshift was observed in the absorption band of the ligands upon dropwise addition of Ti salts which is in favor of the synthesis of catalysts capable of working under visible light. The redshift reflects a decline in the energy bandgap ($\Delta = E(\text{HOMO}) - E(\text{LUMO})$), thus, the shift of wavelength toward the lower energies (visible light). Therefore, the obtained catalysts can absorb visible light. The isosbestic points in the spectra indicate the equilibrium processes of complex formation. The emergence of longer wavelength absorption bands does not contradict the formation of deeply colored complexes isolated from

**Fig. 4.** XRD pattern of M₂L^x.**Table 2**

2θ of the samples obtained from the ligands and complexes.

Compounds	2θ
L ¹	36.46
Ti ^{IV} (L ¹) (OH) ₂ ·H ₂ O	31.105
L ²	14.385, 16.035, 18.385, 21.665, 24.865, 28.395
Ti ^{III} ₂ (L ²)(OH) ₂	18.3, 21.3, 21.8, 29.3, 32.1, 35.2, 37.2, 38.3, 45.3, 55.2, 55.6, 59.1, 62.2, 75.1
Ti ^{IV} ₂ (L ³)Br ₄	–
L ³	11.255, 13.735, 17.395, 18.375, 18.815, 20.855, 22.355, 25.545, 26.965, 27.815, 29.015, 31.065, 33.155
Ti ^{IV} ₂ (L ³) Br ₄ (OH) ₂	25.805, 29.865, 42.725
L ⁴	11.165, 18.195, 18.865, 19.025, 21.945, 22.025, 22.105, 22.165, 22.665, 23.345, 23.455, 26.395, 28.055, 28.155, 28.205, 28.285
Ti ^{IV} (L ⁴)Br ₂	22.045, 22.635, 22.925, 24.585, 29.435, 30.075
L ⁵	16.095, 16.795, 17.775, 19.735, 21.475, 22.885, 23.605, 25.205, 27.305, 30.235
Ti ^{IV} (L ⁵)Br ₂ (OH)	–
L ⁶	16.775, 20.825, 25.085, 25.325
Ti ^{III} ₂ (L ⁶) Cl ₄ ·9H ₂ O	11.535, 12.745, 18.615, 19.575, 21.025, 22.165, 22.505, 22.715, 23.345, 23.605, 24.005, 24.435, 24.955, 26.105, 27.515, 28.495, 28.725, 31.915, 32.165, 34.185, 38.235, 42.925, 45.545, 46.575, 50.485
L ⁷	14.495, 19.015, 19.815, 24.265
Ti ^{III} (L ⁷) OH·4H ₂ O	15.225, 22.735, 24.395, 27.305, 28.845, 29.975, 31.215, 34.115, 35.715
(Ti ^{IV} O) ₂ (L ⁷)Br ₂	20.215, 22.165, 23.565, 28.085, 45.355
L ⁸	12.305, 13.625, 15.165, 17.235, 18.315, 20.145, 21.965, 24.145, 24.935, 27.055, 28.305
Ti ^{III} (L ⁸)Cl ₂ ·H ₂ O	–
(Ti ^{IV} O)(L ⁸)Br	20.4252, 24.6199, 25.7431, 26.9657, 27.9299, 28.6257
L ⁹	12.815, 18.415, 19.435, 20.035, 22.005, 24.265, 25.695, 27.045, 31.405
(Ti ^{IV} O) ₂ (L ⁹)Br ₂	–

solutions (see the synthetic part). Table 1 lists the results of UV–vis spectroscopy for all the complexes.

A comparison of the XRD results of L¹–L⁹ with their corresponding Ti^{III} and Ti^{IV} complexes indicated the formation of new phases (Figs. 2–4). The ligand peaks disappeared or shifted in the complexes. Thus, no mixtures of Ti-salts with the organic species were isolated. It must be noted that L¹, Ti^{IV}₂(L²)Br₄ (3), Ti^{IV}(L⁵)Br₂(OH) (6), and (Ti^{IV}O)₂(L⁹)Br₂ (12) did not give reflections in the XRD patterns, i.e. they are amorphous. The XRD results of all complexes are presented in Table 2.

The SEM images of the isolated complexes showed that the majority of the samples have a proper surface area. As an example, Ti^{IV}(L⁵)

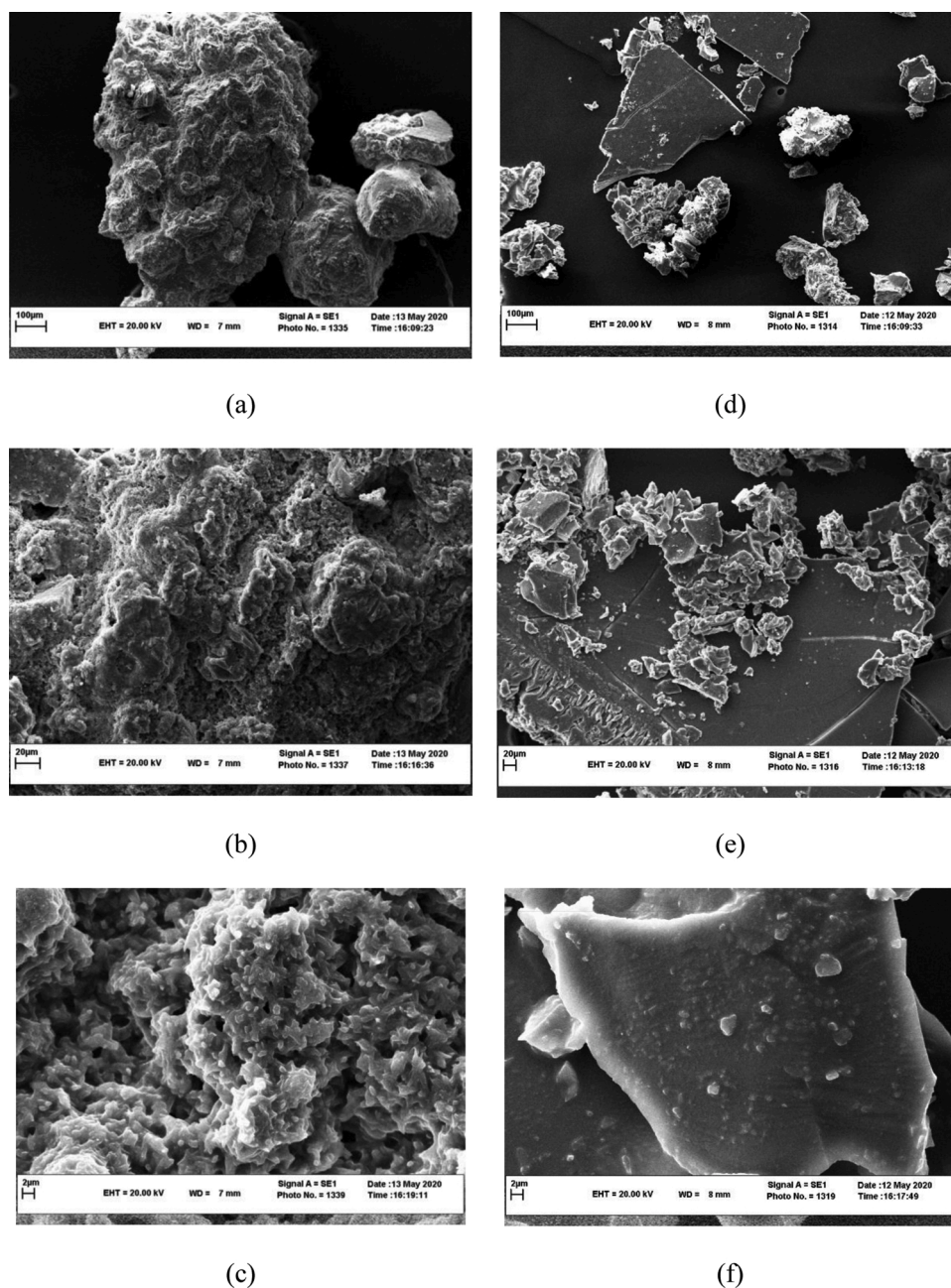


Fig. 5. SEM images of $\text{Ti}^{\text{IV}}(\text{L}^5)\text{Br}_2(\text{OH})$ (a–c) and $(\text{Ti}^{\text{IV}}\text{O})_2(\text{L}^7)\text{Br}_2$ (d–f) at various magnifications.

$\text{Br}_2(\text{OH})$ complex exhibited a highly porous sponge-like structure (Fig. 5) which is attractive for catalytic activities.

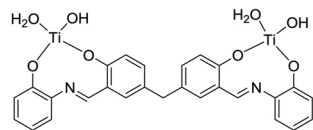
3.2. Spectral characteristics and expected structure of the complexes

In all the cases the complexation of Ti with the organic ligands can be proved by the strong changes in color. In all cases, the shifts are observed in the absorption bands (the color changes to the orange-reddish part of the spectrum) which can be attributed to the formation of new unoccupied molecular orbitals involving Ti atomic orbitals. These orbitals decremented the energy band gap, offering the possibility of visible light absorption.

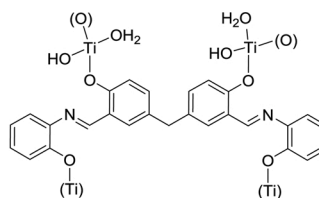
As the single crystal isolation of the complexes failed, the structures of the isolated compounds were predicted from their spectroscopic characteristics.

3.3. L^1 and Ti^{IV} -complex

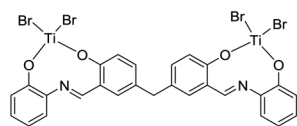
According to the elemental analysis, the composition of the complex can be presented as $\text{Ti}^{\text{IV}}(\text{L}^1)(\text{OH})_2 \cdot \text{H}_2\text{O}$. As NaOH solution was used to increase the solubility of L^1 and acetone used as a solvent, the introduction of OH groups and water molecules into the complex was not unexpected. The ^1H NMR spectrum of the ligand showed a peak at 9.72 ppm which correlates to two protons of the hydroxy groups. No peak was observed in this area for the Ti-complex which may indicate the dissociation of the OH-groups of the ligand upon complexation. The peaks at 2.25–2.12 (m, 2 H) and 2.11 (s, 2 H) ppm can be assigned to the protons of OH groups and H_2O molecule, respectively. The shift in the signal of $\text{H}-\text{C}=\text{N}$ proton at complexation reflects the involvement of N-pyridine in coordination. Thus, the structure of the complex may be presented as (12):



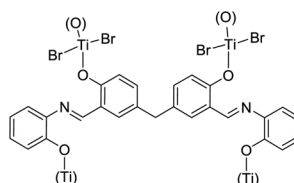
(13a)



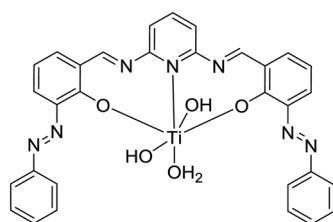
(13b)



(14a)



(14b)



(12)

3.4. L^2 and Ti^{III}/Ti^{IV} -complexes

According to elemental analysis, the composition of the complex compounds can be presented as $Ti^{III}_2(L^2)(OH)_2$ and $Ti^{IV}_2(L^2)Br_4$. The absorption bands of the OH-groups in the IR spectrum of the ligand are observed as a wide band of rather low intensity in the range $3400\text{--}3000\text{ cm}^{-1}$ which overlapped with the C—H aromatic stretches. This absorption band disappeared in the IR spectra of the complexes, indicating the ionization of the OH groups. The $\nu(C\text{--}O)$ band of the ligand at 1275 cm^{-1} shifted to higher frequencies (1282 and 1281 cm^{-1} for Ti^{III} and Ti^{IV} complexes, respectively), implying a decrease in the electron density on O-atoms due to their coordination with Ti-ions.

The 1H NMR spectrum of L^2 is characterized by two signals at 9.72 (2 H) and 13.62 (2 H) ppm which can be assigned to two pairs of non-equivalent hydroxy groups. Two of the OH-groups are involved in strong intramolecular H-bonding, while the other two form the intermolecular H-bonds are associated with the organic molecules in the crystal. No signals were detected above 9 ppm in the 1H NMR spectra of the complexes indicating the ionization of the OH-groups during the complexation.

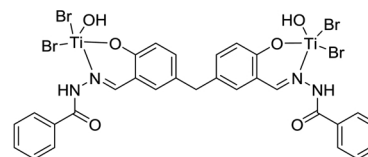
The position of the C—H protons of the C=N fragments of the organic species (8.94 ppm, s, 2 H) does not significantly change upon complexation (8.96 ppm). One can suppose that the N-atoms of the L^2 molecule were not involved in coordination. Based on the coordination number of Ti as 4 and the geometrical features of the organic molecule, two structures ($Ti^{III}_2(L^2)(OH)_2$ and $Ti^{IV}_2(L^2)Br_4$) can be proposed as binuclear monomeric (13a, 13b) or coordination polymer (14b, 14b) in which two of the O-atoms of the terminal fragments of L^2 form coordinate bonds with the Ti atoms of the neighboring monomers.

3.5. L^3 and Ti^{IV} -complex

According to the elemental analysis, the composition of the complex can be presented as $Ti^{IV}_2(L^3)Br_4(OH)_2$. In the IR spectrum of L^3 , the characteristic absorption band of C=O stretching at 1648 cm^{-1} did not shift upon complexation, indicating that the carbonyl groups of the organic ligand are not involved in coordination with Ti. The absorptions at 3205 and 3108 cm^{-1} can be assigned to $\nu(N\text{--}H)$ and $\nu(O\text{--}H)$, respectively. The significant low-frequency shift of the OH bands could be assigned to the strong intramolecular H-interactions with N-atoms of neighboring hydrazo-groups. In the IR spectrum of the complex, the band assigned to the N—H stretches remained unchanged while the $\nu(O\text{--}H)$ absorption bands disappeared. A new broad band at 3460 cm^{-1} in the spectrum of the complex compound indicates the presence of hydroxy-groups attached to the Ti cations.

The 1H spectrum of the L^3 ligand contains the signals at 11.08 (2H, OH) and 12.10 (2H, NH) ppm. The signal at 8.65 ppm (2 H) can be ascribed to two equivalent independent protons of the —HC=N— fragments. Upon the complex formation, the signal at 11.08 ppm disappeared, and the signal of the N—H protons emerged at 11.48 ppm indicating the involvement of neighboring N atoms of two hydrazo-groups in coordination. Together, the signal of the —HC=N— fragments shifted to 8.51 ppm. The appearance of a signal at 2.10 ppm in the spectrum of $Ti_2(L^3)Br_4(OH)_2$ can be assigned related to two OH-groups in the inner sphere of the Ti cations.

Summarizing all the abovementioned discussions and considering that the coordination numbers of Ti(IV) can be 4, 5, or 6, the following structure can be proposed (15).



(15)

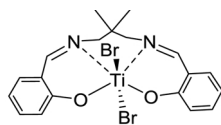
3.6. L^4 and Ti^{IV} -complex

The elemental analysis indicates that the Ti-to- L^4 ratio in the complex is ranged from 1 to -1. The formula can be presented as $Ti^{IV}(L^4)Br_2$. No characteristic absorption bands can be observed in the IR spectra of both L^4 and its Ti complex. In the 1H NMR spectrum of the organic species, two protons of the OH groups (13.60 ppm) and two protons of the

Table 3
Selected calculated parameters for $L^1 - L^9$.

Compound	E(HOMO), eV	E(LUMO), eV	ΔE , eV	Dipole moment, Debye
L^1	-8,2353	-0,9745	7,2608	4,63
L^2	-8,2016	-0,3371	7,8645	3,49
L^3	-8,1781	0,1732	8,3513	2,32
L^4	-8,4374	0,3462	8,7836	4,46
L^5	-9,2868	0,3244	9,6112	5,46
L^6	-7,9075	-0,1888	7,7187	1,59
L^7	-8,5569	0,6304	9,1873	3,32
L^8	-7,9459	-0,3403	7,6056	4,78
L^9	-7,9717	-0,2970	7,6747	0,08

the $-\text{HC}=\text{N}-$ fragments (8.38 ppm) can be observed. In the spectrum of $\text{Ti}(\text{L}^4)\text{Br}_2$, the signal of OH groups is not observed, and the signal of $-\text{HC}=\text{N}-$ fragments shifted to 8.21 ppm indicating the involvement of N-atoms in coordination with titanium. The proposed structure of the complex compound is presented below (16):

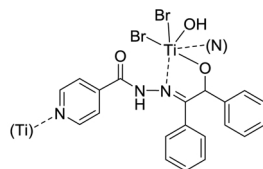


(16)

Ti(IV) atom is six coordinated and forms a distorted octahedral coordination sphere where two Br atoms act as azimuthal ligands.

3.7. L^5 and its Ti^{IV} complex

The composition of the Ti-complex compound of L^5 is $\text{Ti}(\text{L}^5)\text{Br}_2(\text{OH})$; implying the existence of organic ligand in the form of mono-anion. Comparison of the IR spectra of L^5 and its complex indicated no shift of the absorption band of the $\text{C}=\text{O}$ group (1676 cm^{-1} in L^5 vs 1680 cm^{-1} in $\text{Ti}^{\text{IV}}(\text{L}^5)\text{Br}_2(\text{OH})$). Thus, the $\text{C}=\text{O}$ group is not involved in coordination. The structure of the complex compound can be presented as:

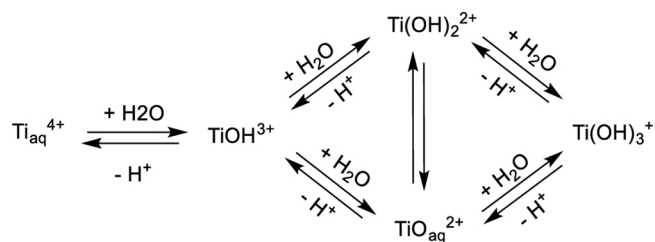


(17)

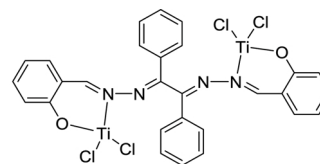
The N-atom of the pyridine fragment of the organic ligand may form an additional coordination bond with a Ti atom of a neighboring molecule; resulting in the formation of a polymeric structure.

3.8. L^6 and its Ti complex

$\text{Ti}^{\text{III}}_2(\text{L}^6)\text{Cl}_4 \cdot 9\text{H}_2\text{O}$ is the formula of the complex derived from the elemental analysis. Nine lattice water molecules indicate strong hygroscopic properties of the substance. In the IR spectrum of the complex, their vibration appeared as a wide strong absorption in $3380\text{--}3200 \text{ cm}^{-1}$ which overlapped with the area of OH stretchings of L^6 (3250 cm^{-1}). However, the absence of the signals of protons at 10.90 (s, 1H, OH) and 9.03 (s, 1H, OH) ppm in the spectrum of $\text{Ti}^{\text{III}}_2(\text{L}^6)\text{Cl}_4 \cdot 9\text{H}_2\text{O}$ showed the ionization of the ligand upon complexation. The structure of coordination of L^6 in the Ti^{III} complex can be presented as (18):



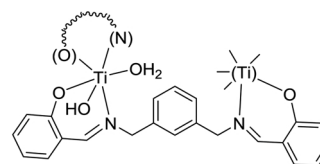
Scheme 1. Formation of titanyl ions at complex formation.



(18)

3.9. L^7 and Ti^{III} / Ti^{IV} complexes

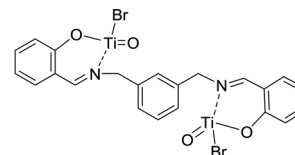
Determination of the molecular structure of complexes in the absence of a single crystal was done by DFT optimizations in the gas phase of the ligands (Fig. 4). Selected energetic and geometrical parameters of $L^1 - L^9$ are presented in Table 3.



(19)

According to the elemental analysis, the composition of the complex compound of Ti^{IV} with L^7 is related to the formula $(\text{Ti}^{\text{IV}}\text{O})_2(\text{L}^7)\text{Br}_2$. The presence of the titanyl fragment $(\text{TiO})^{2+}$ can be predicted using IR spectra. New adsorption bands at 900 cm^{-1} ($\nu(\text{Ti}=\text{O})$) and $660/625 \text{ cm}^{-1}$ ($\nu(\text{Ti}-\text{O})$) appear in the spectrum of the complex compared to that of the ligand. The formation of titanyl ions upon complexation is in accordance with the scheme of the hydrolysis of Ti(IV) ions proposed by Comba & Metbach (Scheme 1) [84]:

The dissociation of the two hydroxy-groups of L^7 upon complexation is manifested as the signals of two protons at 13.45 ppm on the ^1H NMR spectrum of the ligand which is not observable in the case of $(\text{Ti}^{\text{IV}}\text{O})_2(\text{L}^7)\text{Br}_2$. The signal of two protons of the $-\text{HC}=\text{N}-$ fragment in the organic species at 8.73 ppm (2 H) shifted to 8.32 ppm (5 H) upon complexation and overlapped with the signals of the protons of benzene rings of the organic molecule, indicating the involvement of N-lone electron pairs in coordination with Ti(IV). As a result, the structure of the complex compound can be presented as (20):



(20)

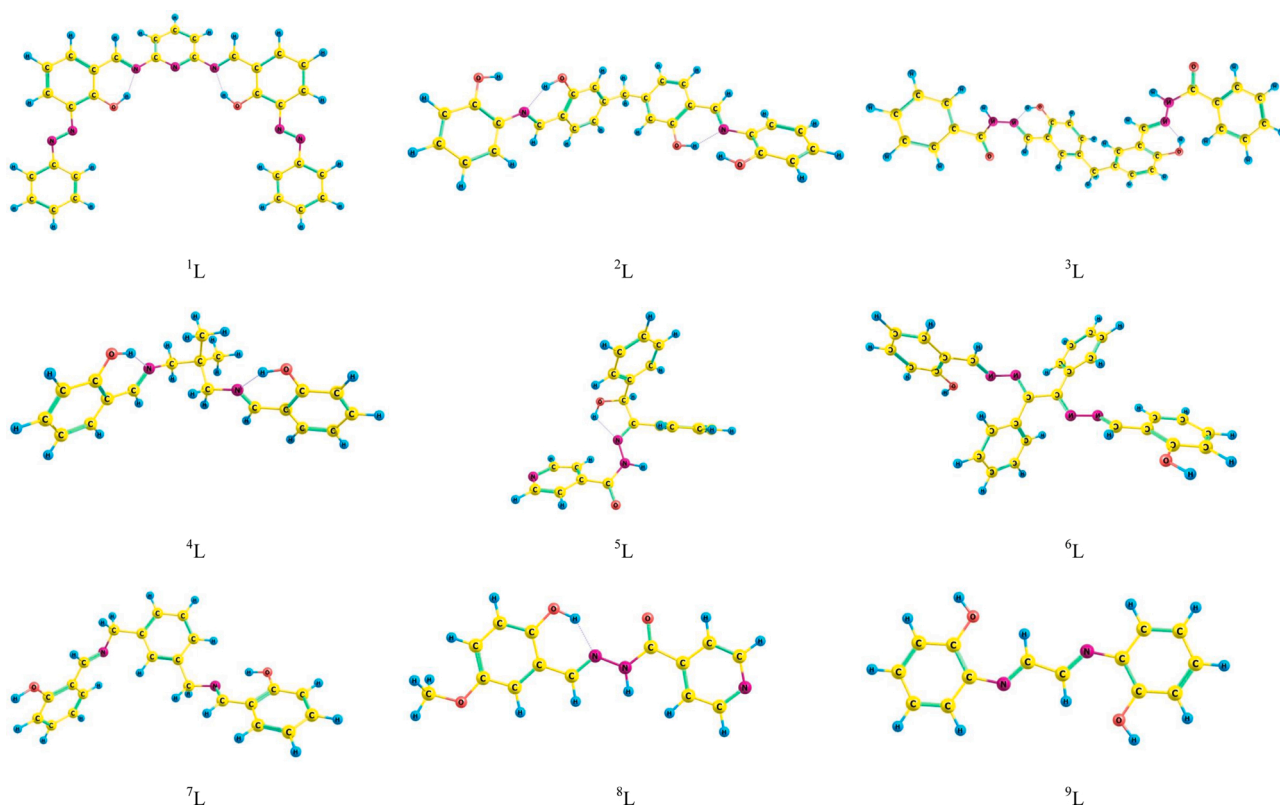


Fig. 6. DFT optimized structures of $L^1 - L^9$.

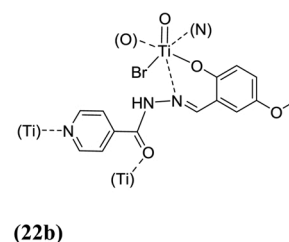
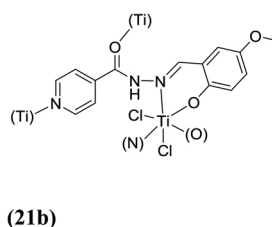
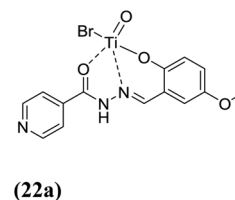
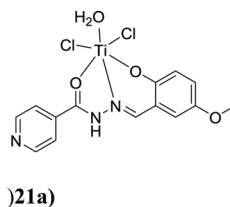
3.10. L^8 and Ti^{III}/Ti^{IV} complexes

In the IR spectrum of the ligand, a broad absorption at $3434-3300\text{ cm}^{-1}$ ($\nu(\text{O}-\text{H} + \text{N}-\text{H})$) got sharper upon complexation with a maximum at 3329 and 3380 cm^{-1} ($\nu(\text{N}-\text{H})$) for $Ti^{III}(L^8)Cl_2 \cdot H_2O$ and $(Ti^{IV}O)(L^8)Br$, respectively. This may be due to the ionization of hydroxy groups. A comparison of the ^1H NMR spectra of the complexes with the free (non-complexed) ligand showed that the signal of two protons of the hydroxy-groups (at 10.62 ppm) disappeared while the signal of the protons of the NH-groups at 12.33 ppm was observed in both spectra.

The absorption band of the $\text{C}=\text{O}$ group in the IR spectrum of the ligand (1653 cm^{-1}) shifted to a lower frequency (1635 and 1642 cm^{-1}) for $Ti^{III}(L^8)Cl_2 \cdot H_2O$ and $(Ti^{IV}O)(L^8)Br$ upon complexation, indicating the formation of a coordinate bond with the Ti^{III} and Ti^{IV} cations. The formation of a titanyl fragment ($\text{TiO})^{2+}$ in the complex of Ti^{IV} can be inferred by the emergence of a new adsorption band at 914 cm^{-1} ($\nu(\text{Ti}=\text{O})$).

Based on the spectral characteristics of the complex compared with the uncoordinated L^8 , two possible types of coordination can be proposed.

In the first type, L^8 acts as a tridentate ligand to form monomeric mononuclear complexes of **21a** and **22a**. In the second case, L^8 serves as a tridentate bridging ligand where the $\text{C}=\text{O}$ group of one ligand molecule forms a coordinate bond with a Ti atom of a neighboring monomer. The N-pyridine atom can be also involved in coordination, giving rise to 3D polymeric structures (**21b** and **22b**). Thus, the structures of the complex may be presented as:



3.11. L^9 and Ti^{IV} complex

According to the elemental analysis, the formula of the complex compound is $(Ti^{IV}O)_2(L^9)Br_2$. In the IR spectrum of the ligand, a broad absorption is observed with a maximum at 3384 cm^{-1} ($\nu(\text{O}-\text{H})$). In the spectrum of the complex, no band was observed in this region, implying the dissociation of OH groups of the ligand. The titanyl group vibrations in the IR spectrum of the complex corresponded to 902 cm^{-1} .

The ^1H NMR spectrum of the ligand shows the signal of two protons of hydroxy groups at 9.93 ppm which disappeared upon complexation. The proposed structure of the complex can be presented as following (**23**):

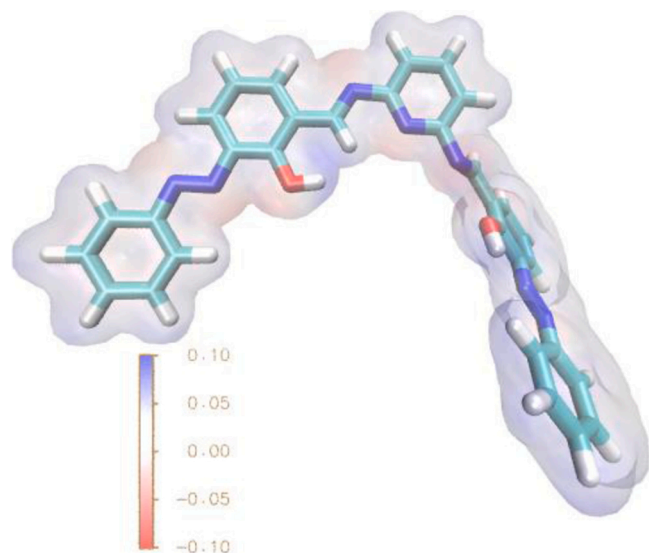
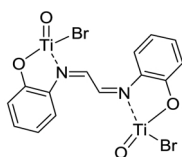


Fig. 7. Molecular electrostatic potential (MESP) of L^1 .



(23)

3.12. Theoretical simulations

The molecular structure of complexes was determined by DFT optimizations in the gas phase of the ligands (Fig. 6). The energetic and geometrical parameters of L^1 – L^9 are presented in Table 3

Molecular electrostatic surface potential (MESP) charge regionalization was set up by electron density plot. As an example, the MESP potential of L^1 is presented in Fig. 7 which indicates that the O atoms of hydroxy groups possess a negative potential region, i.e. are the most preferable coordination sites of the ligand. Similar results were reported by Shukla et al. for the Schiff base complexes of titanocene dichloride [85].

The spatial arrangement of the electron-donating fragments of the molecules (L^1 – L^9) is in line with the proposed structures of the complexes derived from the spectral studies. For example, in the case of Ti-complexes with L^2 , phenolic groups of neighboring phenolic fragments are in the *syn*-position. Thus, monomeric binuclear complexes of 13a and 14a seem to be more preferable than polymeric 13b and 14b structures. The complexes with bis(tridentate) coordination of L^2 via two oxygens of deprotonated OH groups and an N atom of the $-\text{HC}=\text{N}-$ fragment are in lower energy levels compared to bis(bidentate) coordination

involving only O-atoms (Table 4).

DFT optimization of the $(\text{Ti}^{\text{IV}}\text{O})_2(\text{L}^7)\text{Br}_2$ structure is presented in Fig. 8. The $\text{Ti}^{\text{IV}}=\text{O}$ bond length was determined as 1.6 Å reflecting its double character. The IR spectrum simulation resulted in 994 cm^{-1} and 626 cm^{-1} for $\nu(\text{Ti}=\text{O})$ and $\nu(\text{Ti}-\text{O})$, respectively which well coincided with the experimental IR spectrum of $(\text{Ti}^{\text{IV}}\text{O})_2(\text{L}^7)\text{Br}_2$ (Fig. 9). The spectrum of the complex showed absorption peaks at 900 and $660/625\text{ cm}^{-1}$ which are not observed in the spectrum of L^7 .

4. Photocatalytic activity of complexes as catalysts in the C–N cross-coupling reaction

To evaluate the photocatalytic efficiency of the obtained complexes, they were used in the C–N cross-coupling. The catalytic activity of the complexes was investigated in the Buchwald–Hartwig reaction. For this purpose, the cross-coupling reaction between bromobenzene and aniline was considered as a model reaction. To better estimate the reaction condition, the effects of the different parameters such as solvent, base, the molar ratio of bromobenzene, base, and catalyst were first examined. The data corresponding to $\text{Ti}^{\text{III}}(\text{L}^8)\text{Cl}_2\cdot\text{H}_2\text{O}$ (M_1L^8) can be found in Table 5. The photocatalytic activity and reaction conditions are summarized in Table 5.

According to the result, the reaction did not occur in the absence of a catalyst or base for any types of catalysts. These results confirmed the photocatalytic nature of the complexes showing the necessity of both base and catalyst for the C–N cross-coupling reaction (Table 5, entries 1–3). In the second screening experiment, the effects of various solvent systems were investigated. For this purpose, different polar/non-polar solvents (such as DMSO, DMF, THF, DCM, toluene, CH_3CN , EtOH,

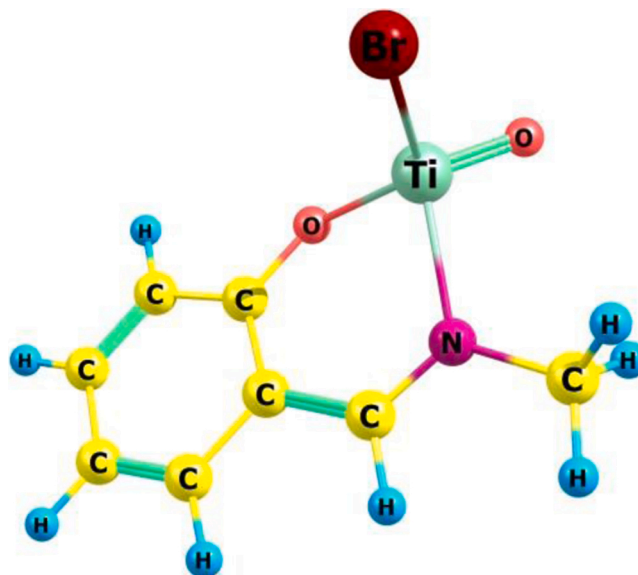


Fig. 8. DFT optimization of $(\text{Ti}^{\text{IV}}\text{O})_2(\text{L}^7)\text{Br}_2$.

Table 4

Relative energies of bis(bidentate) and bis(tridentate) coordination of L^2 (only one coordination fragment is considered for clarity).

$\Delta E, \text{ kJ/mol}$	
0	86.62

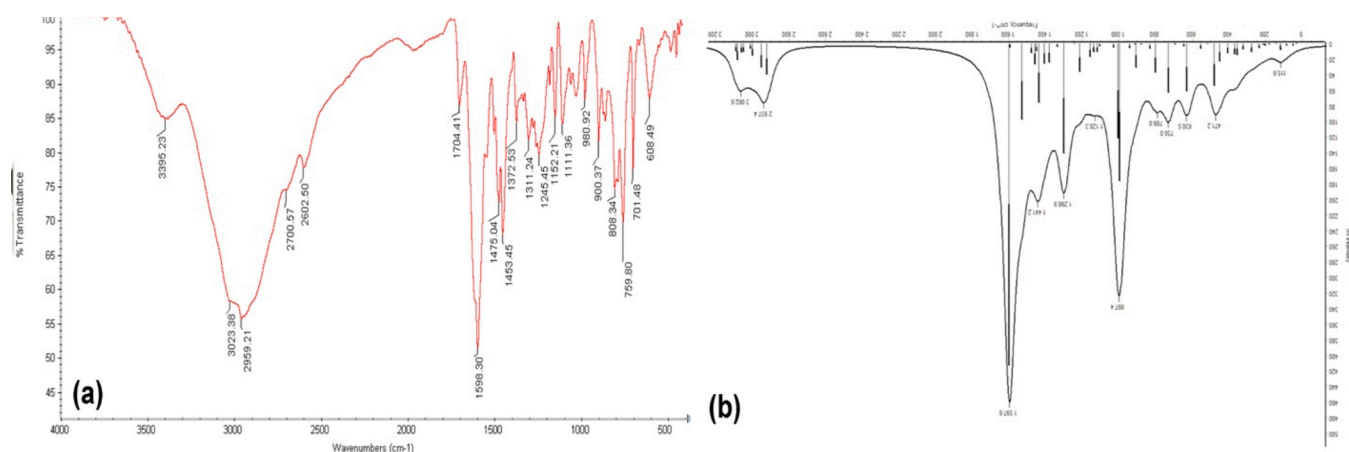


Fig. 9. IR spectrum of $(\text{Ti}^{\text{IV}}\text{O})_2(\text{L}^7)\text{Br}_2$ (a); calculated for $(\text{Ti}^{\text{IV}}\text{O})_2(\text{L}^7)\text{Br}_2$ (b).

Table 5

Optimization of the reaction conditions for coupling reaction.



Entry	Catalyst (mol%) ^c	Base	Solvent	Molar ratio of Bromobenzene/Base	Time (h)	Isolated Yield (%) ^{a,b}
1	–	–	DMF	1/0	24	0 ^a
2	–	K ₂ CO ₃	DMF	1/1	24	0 ^a
3	0.4	–	DMF	1/0	24	0 ^a
4	0.4	K ₂ CO ₃	DMF	1/1	24	0 ^b
5	0.4	K ₂ CO ₃	DMF	1/1	4	84 ^a
6	0.4	K ₂ CO ₃	DMSO	1/1	4	84 ^a
7	0.4	K ₂ CO ₃	EtOH	1/1	10	40 ^a
8	0.4	K ₂ CO ₃	EtOH-DMF(9:1)	1/1	8	45 ^a
9	0.4	K ₂ CO ₃	H ₂ O	1/1	24	Trace ^a
10	0.4	K ₂ CO ₃	EtOH-H ₂ O(9:1)	1/1	24	23 ^a
11	0.4	K ₂ CO ₃	THF	1/1	10	35 ^a
12	0.4	K ₂ CO ₃	DCM	1/1	6	45 ^a
13	0.4	K ₂ CO ₃	CH ₃ CN	1/1	6	65 ^a
14	0.4	K ₂ CO ₃	MeOH	1/1	8	60 ^a
15	0.4	K ₂ CO ₃	Toluene	1/1	10	30 ^a
16	0.4	KOH	DMF	1/1	5	75 ^a
17	0.4	NaOH	DMF	1/1	5	75 ^a
18	0.4	NEt ₃	DMF	1/1	6	68 ^a
19	0.4	K ₃ PO ₄	DMF	1/1	8	45 ^a
20	0.4	NaHCO ₃	DMF	1/1	8	40 ^a
21	0.4	K ₂ CO ₃	DMF	1/2	4	84 ^a
22	0.4	K ₂ CO ₃	DMF	1/0.5	5	60 ^a
23	0.2	K ₂ CO ₃	DMF	1/1	6	67 ^a
24	0.6	K ₂ CO ₃	DMF	1/1	4	80 ^a
25	0.4	K ₂ CO ₃	DMF	1/1	4	84 ^c
26	0.4	K ₂ CO ₃	DMF	1/1	4	84 ^d

^a Under sunlight irradiation.

^b In the dark.

^c Under 30 W LED irradiation.

^d Under UV irradiation.

^e With respect to bromobenzene.

EtOH-DMF, EtOH-H₂O, MeOH, and H₂O) were studied (Table 5, entries 5–15). Among the examined solvents, DMF was the best medium with the highest diphenylamine yield (84 %), thus, it was considered for other catalysts. H₂O resulted in the lowest yield of diphenylamine (Table 5, entries 5 and 9). Further control experiments were performed regarding the role of bases on the yield of the C-N cross-coupling reaction. Therefore, the model reaction was carried out considering different bases, including K₂CO₃, KOH, NaOH, NEt₃, K₃PO₄, and NaHCO₃, (Table 5, entries 5, 16–20). It was found that K₂CO₃ led to a higher yield (Table 5, entry 5). Then, the amount of base was also explored. Based on these results, using 1 equivalent of base proceeded the cross-coupling reaction very effectively (Table 5, entries 5, 21, and 22). There were

no differences in the yield and reaction time between 1 and 2 equivalents of K₂CO₃. While a decline in the amount of base decremented the yield of the desired product and prolonged the reaction time (Table 5, entry 22). The photocatalyst amount was also optimized. The best performance was achieved by applying 0.0016–0.0024 g of the catalysts. As the final control reaction, it was verified that when the reaction was performed in the dark no catalytic reaction was detected (Table 5, entry 4).

To confirm the excellent sunlight applicability of the photocatalyst, the optimized reaction condition was tested using different light sources including blue 30 W LED lamp, 100 W Hg lamp (UVA, UVB Light), and natural sunlight (Table 5, entry 5, 25, and 26). As shown in Table 5, blue

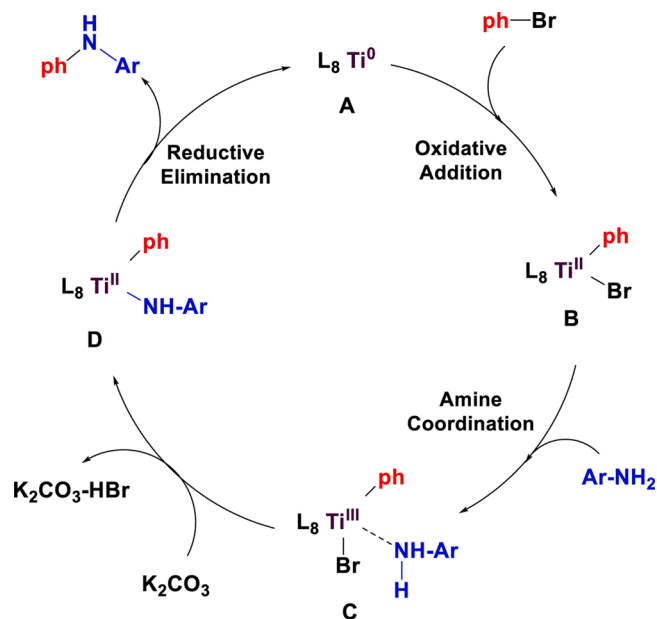
Table 6
Scope of the C-N cross coupling reaction.

Entry	Catalyst	R	Product	Time (h)	Isolated Yield (%)
1	M ₂ L ¹			4	84
2	M ₁ L ²			6	72
3	M ₂ L ²			6	78
4	M ₂ L ³			7	65
5	M ₂ L ⁴			4	84
6	M ₂ L ⁵			8	65
7	M ₁ L ⁶			5	84
8	M ₁ L ⁷			8	58
9	M ₂ L ⁷			5	79
10	M ₁ L ⁸			8	50
11	M ₂ L ⁸			3	75
12	M ₂ L ⁹			4	81

Reaction conditions: bromobenzene (1.0 mmol), Amine derivatives (1.0 mmol), K₂CO₃ (1 mmol), DMF (4.0 mL), Catalyst (0.0016 g) under sunlight at ambient temperature.

30 W LED, Hg lamp, and sunlight showed the same results, so visible sunlight was chosen for further investigations. Finally, the C-N cross-coupling reaction was studied using all the catalysts on a sunny day, in July, in Mashhad between 10 am to 5 pm at the temperature ranges of 22–34 °C.

Almost all the complexes showed their best activity in the same conditions, so to evaluate the generality and substrate role, the photocatalytic activity was further explored under optimized reaction condition considering C-N cross-coupling reaction with a variety substituted aromatic amines using K₂CO₃ as a base in DMF at room temperature under natural sunlight (Table 6). As shown in Table 6, the reaction efficiently proceeded with a wide range of electron-withdrawing and electron-donating substituents. The results showed that both electron-withdrawing (Table 6, entry 1–8,11) and donating group (Table 6, entry 9 and 12) were delivered to the corresponding secondary aromatic amines at moderate to good yields (50–84 %). Comparatively, as expected, aryl-bearing electron-withdrawing groups reacted significantly faster than those containing electron-donating groups. Furthermore, owing to the high steric hindrance of the ortho position, substituents in the ortho position of amines show low reactivity as compared to the para one (Table 6, entry 5 and 6). It is worth noting that different catalysts were applied for different reactions to test different reactions.



Scheme 2. Mechanism for M₁L⁸ catalysed C-N cross coupling reaction.

5. Proposed mechanism

Based on some previous reports [86–88], a proposed mechanism was proposed for catalyzing the C-N cross-coupling reaction (Scheme 2). Initially, under visible-light irradiation, electrons and holes of TiO₂ were separated and photo-generated electrons migrated. The catalytic cycle began with the insertion of L₈Ti⁰ into the phenyl-Br bond, yielding to intermediate B. In the following, coordination of an amine group under basic condition resulted in intermediate D. The final product and the reduced form of the catalyst were finally formed in a reductive elimination step.

6. Conclusion

Nine novel Schiff bases were derived from salicylic aldehyde and oxalic aldehyde in this study. The isolated organic species were described by a set of experimental methods (IR, CNMR, HNMR, CHN, SEM, XRD). The molecular structure was also elucidated by DFT optimizations in the gas phase. The molecular electrostatic surface potential (MESP) charge regionalization was set up by electron density plot. The redistribution of the electron density in the organic species indicated their high potential in metal cations chelating with the preferable coordination through O-atoms of the hydroxy-groups of the molecules.

The isolated organic species were applied as the ligands in the reaction of complex formation with titanium (III) chloride and (IV) bromide. 12 novel complexes were precipitated and studied experimentally and theoretically. The solution stability of the complexes was indicated with UV-vis spectroscopic analysis, their formation constants were calculated to be in the range of 6.84–17.32 depending on the nature of the Schiff base ligand. Using the DFT def2-TZVP theoretical method together with the experimental spectroscopic data, the coordination types of the ligands were detected, and the structure of the complexes was proposed. The spatial arrangement of the electron-donating fragments of L¹–L⁹ molecules was in proper accordance with the proposed structures of the complexes derived from the spectral studies.

The isolated Ti-complexes were used in photocatalytic activity in Buchwald-Hartwig amination reactions which showed highly efficient photocatalysis by promoting the C-N cross-coupling reactions using a wide variety of aromatic and benzylic amines to give cross-coupled products at proper yields.

The photocatalytic activity of the isolated complexes was checked in

the C-N cross-coupling reaction under sunlight using different polar/non-polar solvents. The studied complexes exhibited high visible-light photocatalytic activity for a wide range of aromatic and benzylic amines including electron-withdrawing and electron-donating groups offering moderate to good yields (50–85 %). Using an inexpensive, clean, and renewable energy source (sunlight) is the superiority of the developed photocatalytic systems.

The present study offers a promising strategy to design new metal complexes applicable in various photocatalytic organic reactions.

Authorship contributions

Conception and design of study: Yahya Absalan, Nazanin Noroozi Shad, Mostafa Gholizadeh

Acquisition of data: Yahya Absalan, Ghodrath Mahmoudi

Analysis and/or interpretation of data: Yahya Absalan, Pavel Strashnov, Nazanin Noroozi Shad, Olga Kovalchukova, Hossein Sabet Sarvestani

Drafting the manuscript: Yahya Absalan, Olga Kovalchukova, Nazanin Noroozi Shad

Revising the manuscript critically for important intellectual content: Khashayar Ghandi

Approval of the version of the manuscript to be published: Yahya Absalan, Nazanin Noroozi Shad, Mostafa Gholizadeh, Ghodrath Mahmoudi, Hossein Sabet Sarvestani, Pavel Strashnov, Khashayar Ghandi, Olga Kovalchukova.

Declaration of Competing Interest

The authors declare that they have no known competing financial interests or personal relationships that could have appeared to influence the work reported in this paper

Acknowledgement

This paper has been supported by the RUDN University Strategic Academic Leadership Program and the Ferdowsi University of Mashhad research Council

Appendix A. Supplementary data

Supplementary material related to this article can be found, in the online version, at doi:<https://doi.org/10.1016/j.jphotochem.2021.113346>.

References

- P.A. Forero-Cortés, A.M. Haydl, The 25th anniversary of the Buchwald-Hartwig amination: development, applications, and outlook, *Org. Process Res. Dev.* 23 (2019) 1478–1483, <https://doi.org/10.1021/acs.oprd.9b00161>.
- A.J. Kendall, L.N. Zakharov, D.R. Tyler, Steric and electronic influences of Buchwald-type alkyl-JohnPhos ligands, *Inorg. Chem.* 55 (2016) 3079–3090, <https://doi.org/10.1021/acs.inorgchem.5b02996>.
- W.W. Weare, R.R. Schrock, A.S. Hock, P. Müller, Synthesis of molybdenum complexes that contain “hybrid” triamidoamine ligands, [(hexaisopropylterphenyl-NCH₂CH₂)₂NCH₂CH₂N-aryl]₃-, and studies relevant to catalytic reduction of dinitrogen, *Inorg. Chem.* 45 (2006) 9185–9196, <https://doi.org/10.1021/ic0613457>.
- H. Hu, M. Vasilii, T.H. Stein, F. Qu, D.L. Gerlach, D.A. Dixon, K.H. Shaughnessy, Synthesis, structural characterization, and coordination chemistry of (Trineopentylphosphine)palladium(aryl)bromide dimer complexes [(Np₃P)Pd(Ar)Br]₂, *Inorg. Chem.* 58 (2019) 13299–13313, <https://doi.org/10.1021/acs.inorgchem.9b02164>.
- Fluorine in Organic Chemistry - Richard D. Chambers - Google Books, (2004). [https://books.google.com/books?hl=en&lr=&id=XE5VHh7uL0C&oi=fnd&pg=PR15&dq=R.+D.+Chambers,+Fluorine+in+organic+chemistry.+CRC+Press:+2004.+b\)+P.+Kirsch,+Modern+Fluoroorganic+Chemistry:+Synthesis,+Reactivity,+Applications+Wiley.+VCH:+2004.+c\)+K.+Muller,+C.+Faeh,+F.+Diederich,+Fluorine+in+pharmaceuticals:+looking+beyond+intuition&ots=62yTaXRSPQ&sig=NScwLwRym1F9SHrybxE5jEQUcg#v=onepage&q&f=false](https://books.google.com/books?hl=en&lr=&id=XE5VHh7uL0C&oi=fnd&pg=PR15&dq=R.+D.+Chambers,+Fluorine+in+organic+chemistry.+CRC+Press:+2004.+b)+P.+Kirsch,+Modern+Fluoroorganic+Chemistry:+Synthesis,+Reactivity,+Applications+Wiley.+VCH:+2004.+c)+K.+Muller,+C.+Faeh,+F.+Diederich,+Fluorine+in+pharmaceuticals:+looking+beyond+intuition&ots=62yTaXRSPQ&sig=NScwLwRym1F9SHrybxE5jEQUcg#v=onepage&q&f=false) (accessed June 26, 2020).

- D.S. Surry, S.L. Buchwald, Dialkylbiaryl phosphines in Pd-catalyzed amination: a user's guide, *Chem. Sci.* 2 (2011) 27–50, <https://doi.org/10.1039/c0sc00331j>.
- J.F. Hartwig, Approaches to catalyst discovery. New carbon-heteroatom and carbon-carbon bond formation, *Pure Appl. Chem.* 71 (1999) 1417–1423, <https://doi.org/10.1351/pac199971081417>.
- D. Maiti, B.P. Fors, J.L. Henderson, Y. Nakamura, S.L. Buchwald, Palladium-catalyzed coupling of functionalized primary and secondary amines with aryl and heteroaryl halides: two ligands suffice in most cases, *Chem. Sci.* 2 (2011) 57–68, <https://doi.org/10.1039/c0sc00330a>.
- J.F. Hartwig, Evolution of a fourth generation catalyst for the amination and thioetherification of aryl halides, *Acc. Chem. Res.* 41 (2008) 1534–1544, <https://doi.org/10.1021/ar800098p>.
- J.P. Wolfe, S. Wagaw, J.F. Marcoux, S.L. Buchwald, Rational development of practical catalysts for aromatic carbon-nitrogen bond formation, *Acc. Chem. Res.* 31 (1998) 805–818, <https://doi.org/10.1021/ar9600650>.
- J.F. Hartwig, Transition metal catalyzed synthesis of arylamines and aryl ethers from aryl halides and triflates: scope and mechanism, *Angew. Chemie Int. Ed.* 37 (1998) 2046–2067, [https://doi.org/10.1002/\(SICI\)1521-3773\(19980817\)37:15<2046::AID-ANIE2046>3.0.CO;2-L](https://doi.org/10.1002/(SICI)1521-3773(19980817)37:15<2046::AID-ANIE2046>3.0.CO;2-L).
- D.S. Surry, S.L. Buchwald, Biaryl phosphane ligands in palladium-catalyzed amination, *Angew. Chemie - Int. Ed.* 47 (2008) 6338–6361, <https://doi.org/10.1002/anie.200800497>.
- J.J. Carbó, D. García-López, O. González-Del Moral, A. Martín, M. Mena, C. Santamaría, Carbon-nitrogen bond construction and carbon-oxygen double bond cleavage on a molecular titanium oxonitride: a combined experimental and computational study, *Inorg. Chem.* 54 (2015) 9401–9412, <https://doi.org/10.1021/acs.inorgchem.5b00943>.
- C. Paparizos, J.P. Fackler, Kinetic studies by NMR of carbon-nitrogen and carbon-oxygen bond rotations in dithiocarbamate and aryl xanthate complexes of dimethylgold(III), *Inorg. Chem.* 19 (1980) 2886–2889, <https://doi.org/10.1021/ic50212a007>.
- J.S. Carey, D. Laffan, C. Thomson, M.T. Williams, Analysis of the reactions used for the preparation of drug candidate molecules, *Org. Biomol. Chem.* 4 (2006) 2337–2347, <https://doi.org/10.1039/b602413k>.
- C. Torborg, M. Beller, Recent applications of palladium-catalyzed coupling reactions in the pharmaceutical, agrochemical, and fine chemical industries, *Adv. Synth. Catal.* 351 (2009) 3027–3043, <https://doi.org/10.1002/adsc.200900587>.
- W.S. Lo, W.M. Kwok, G.L. Law, C.T. Yeung, C.T.L. Chan, H.L. Yeung, H.K. Kong, C. H. Chen, M.B. Murphy, K.L. Wong, W.T. Wong, Impressive europium red emission induced by two-photon excitation for biological applications, *Inorg. Chem.* 50 (2011) 5309–5311, <https://doi.org/10.1021/ic102465j>.
- P. Roy, K. Dhara, M. Manassero, J. Ratha, P. Banerjee, Selective fluorescence zinc ion sensing and binding behavior of 4-methyl-2,6-bis((phenylmethyl)imino)methylphenol: biological application, *Inorg. Chem.* 46 (2007) 6405–6412, <https://doi.org/10.1021/ic700420w>.
- J. Song, T. Jiang, T. Guo, L. Liu, H. Wang, T. Xia, W. Zhang, X. Ye, M. Yang, L. Zhu, R. Xia, X. Xu, Facile synthesis of water-soluble Zn-doped AgIn₅S₈/ZnS core/shell fluorescent nanocrystals and their biological application, *Inorg. Chem.* 54 (2015) 1627–1633, <https://doi.org/10.1021/ic502600u>.
- J. Xie, S. Cao, D. Good, M. Wei, X. Ren, Combination of a fluorescent dye and a Zn-S cluster and its biological application as a stain for bacteria, *Inorg. Chem.* 49 (2010) 1319–1321, <https://doi.org/10.1021/ic9023629>.
- D.A. Horton, G.T. Bourne, M.L. Smythe, The combinatorial synthesis of bicyclic privileged structures or privileged substructures, *Chem. Rev.* 103 (2003) 893–930, <https://doi.org/10.1021/cr020033s>.
- J.A. Bikker, N. Brooijmans, A. Wissner, T.S. Mansour, Kinase domain mutations in cancer: implications for small molecule drug design strategies, *J. Med. Chem.* 52 (2009) 1493–1509, <https://doi.org/10.1021/jm8010542>.
- A. Quintás-Cardama, H. Kantarjian, J. Cortes, Flying under the radar: the new wave of BCR-ABL inhibitors, *Nat. Rev. Drug Discov.* 6 (2007) 834–848, <https://doi.org/10.1038/nrd2324>.
- S.J. Brickner, D.K. Hutchinson, M.R. Barbachyn, P.R. Manninen, D.A. Ulanowicz, S. A. Garmon, K.C. Grega, S.K. Hendges, D.S. Toops, C.W. Ford, G.E. Zurenko, Synthesis and antibacterial activity of U-100592 and U-100766, two oxazolidinone antibacterial agents for the potential treatment of multidrug-resistant gram-positive bacterial infections, *J. Med. Chem.* 39 (1996) 673–679, <https://doi.org/10.1021/jm9509556>.
- J.W. Nilsson, F. Thorstenson, I. Kvarnström, T. Oprea, B. Samuelsson, I. Nilsson, Solid-phase synthesis of libraries generated from a 4-phenyl-2-carboxy-piperazine scaffold, *J. Comb. Chem.* 3 (2001) 546–553, <https://doi.org/10.1021/cc010013o>.
- A.Ç. Atesin, S.B. Duckett, C. Flaschenriem, W.W. Brennessel, R. Eisenberg, Diastereoselective oxidative addition of dihydrogen to Ir(CO)(R)-BINAP and [Ir(CO)₂(R)-BINAP][SbF₆], *Inorg. Chem.* 46 (2007) 1196–1204, <https://doi.org/10.1021/ic061471a>.
- Z. Abedin-Siddique, T. Ohno, K. Nozaki, T. Tsubomura, Intense fluorescence of metal-to-ligand charge transfer in [Pt(0)(binap)₂] [binap = 2,2'-Bis(diphenylphosphino)-1,1'-binaphthyl], *Inorg. Chem.* 43 (2004) 663–673, <https://doi.org/10.1021/ic034527z>.
- T.J. Geldbach, F. Breher, V. Gramlich, P.G.A. Kumar, P.S. Pregosin, X-ray diffraction and NMR studies on a series of binap-based Ru(II) hydroxyphosphine π-Arene complexes, *Inorg. Chem.* 43 (2004) 1920–1928, <https://doi.org/10.1021/ic0352147>.
- T. Ohta, H. Takaya, R. Noyori, BINAP-ruthenium(II) dicarboxylate complexes: new, highly efficient catalysts for asymmetric hydrogenations, *Inorg. Chem.* 27 (1988) 566–569, <https://doi.org/10.1021/ic00276a025>.

- [30] U. Casellato, B. Corain, B. Longato, R. Graziani, G. Pilloni, Heteropolymetallic complexes of 1,1'-Bis(diphenylphosphino)ferrocene (dppf). 5. Synthesis and characterization of the cationic complexes $[\text{M}(\text{dppf})_2]^+$ (M = Rh, Ir). Crystal and molecular structure of $[\text{Ir}(\text{dppf})_2](\text{C}_6\text{H}_5)_4$, *Inorg. Chem.* 29 (1990) 1193–1198, <https://doi.org/10.1021/ic00331a017>.
- [31] B. Longato, L. Riello, G. Bandoli, G. Pilloni, Iridium(III), 0, and -I complexes stabilized by 1,1'-Bis(diphenylphosphino)ferrocene (dppf): synthesis and characterization. crystal structures of $[\text{Na}(\text{THF})_5][\text{Ir}(\text{dppf})_2]^+$ and $[\text{Ir}(\text{dppf})_2]^+$, *Inorg. Chem.* 38 (1999) 2818–2823, <https://doi.org/10.1021/ic981166s>.
- [32] F. Canales, M.C. Gimeno, P.G. Jones, A. Laguna, C. Sarroca, Substitution reaction studies on $[\text{Au} 2 \text{Cl} 2 (\mu\text{-dppf})]$ (dppf = 1,1'-Bis(diphenylphosphino)ferrocene). Synthesis of the first gold(I) complex with a μ 3-2-pyridinethiolate ligand, *Inorg. Chem.* 36 (1997) 5206–5211, <https://doi.org/10.1021/ic970444s>.
- [33] M.C. Gimeno, A. Laguna, C. Sarroca, P.G. Jones, 1,1'-Bis(diphenylphosphino)ferrocene (dppf) complexes of gold(I) and gold(III). Crystal structures of $[(\text{dppf})\text{AuPh}_3]\text{ClO}_4\cdot\text{CHCl}_3$ and $[(\text{dppf})\text{Au}(\mu\text{-dppf})\text{Au}(\text{dppf})](\text{ClO}_4)_2\cdot 2\text{CH}_2\text{Cl}_2$, *Inorg. Chem.* 32 (1993) 5926–5932, <https://doi.org/10.1021/ic00078a007>.
- [34] G. Pilloni, A. Toffoletti, G. Bandoli, B. Longato, Homoleptic complexes of cobalt(0) and nickel(0,I) with 1,1'- bis(diphenylphosphino)ferrocene (dppf): synthesis and characterization, *Inorg. Chem.* 45 (2006) 10321–10328, <https://doi.org/10.1021/ic061185z>.
- [35] M.A. Esteruelas, M. Oliván, A. Vélez, Xantphos-type complexes of group 9: rhodium versus iridium, *Inorg. Chem.* 52 (2013) 5339–5349, <https://doi.org/10.1021/ic4002658>.
- [36] A. Escalle, G. Mora, F. Gagosz, N. Mézailles, X.F. Le Goff, Y. Jean, P. Le Floch, Cationic dimetallic gold hydride complex stabilized by a xantphos-phosphole ligand: synthesis, X-ray crystal structure, and density functional theory study, *Inorg. Chem.* 48 (2009) 8415–8422, <https://doi.org/10.1021/ic901014r>.
- [37] P.A. Mane, S. Dey, A.K. Pathak, M. Kumar, N. Bhuvanesh, Xantphos-capped Pd(II) and Pt(II) macrocycles of arylidithiolates: structural variation and catalysis in C-C coupling reaction, *Inorg. Chem.* 58 (2019) 2965–2978, <https://doi.org/10.1021/acs.inorgchem.8b02726>.
- [38] A.E.W. Ledger, A. Moreno, C.E. Ellul, M.F. Mahon, P.S. Pregosin, M.K. Whittlesey, J.M.J. Williams, Pincer phosphine complexes of ruthenium: formation of $\text{Ru}(\text{P}(\text{O})\text{P})(\text{PPh}_3)_2\text{HCl}$ (P-O-P = xantphos, DPEphos, $(\text{Ph}_2\text{PCH}_2\text{CH}_2)_2\text{O}$) and $\text{Ru}(\text{dppf})(\text{PPh}_3)\text{HCl}$ and characterization of cationic dioxygen, dihydrogen, dinitrogen, and arene coordinated phosphine products, *Inorg. Chem.* 49 (2010) 7244–7256, <https://doi.org/10.1021/ic100438d>.
- [39] D.J. Fox, S.B. Duckett, C. Flaschenriem, W.W. Brennessel, J. Schneider, A. Gunay, R. Eisenberg, A model iridium hydroformylation system with the large bite angle ligand xantphos: reactivity with parahydrogen and implications for hydroformylation catalysis, *Inorg. Chem.* 45 (2006) 7197–7209, <https://doi.org/10.1021/ic060731l>.
- [40] H. Nie, Y. Zhu, X. Hu, Z. Wei, L. Yao, G. Zhou, P. Wang, R. Jiang, S. Zhang, Josiphos-type binaphane Ligands for iridium-catalyzed enantioselective hydrogenation of 1-aryl-substituted dihydroisoquinolines, *Org. Lett.* 21 (2019) 8641–8645, <https://doi.org/10.1021/acs.orglett.9b03251>.
- [41] Q. Shen, T. Ogata, J.F. Hartwig, Highly reactive, general and long-lived catalysts for palladium-catalyzed amination of heteroaryl and aryl chlorides, bromides, and iodides: scope and structure-activity relationships, *J. Am. Chem. Soc.* 130 (2008) 6586–6596, <https://doi.org/10.1021/ja077074w>.
- [42] J. Meng, M. Gao, H. Lv, X. Zhang, Highly enantioselective hydrogenation of o-alkoxy tetrasubstituted enamides catalyzed by a Rh/(R, S)-josiphos catalyst, *Org. Lett.* 17 (2015) 1842–1845, <https://doi.org/10.1021/acs.orglett.5b00401>.
- [43] A.T. Lindhardt, T.M. Gøsgig, T. Skrydstrup, Studies on the 1,2-migrations in Pd-catalyzed Negishi couplings with Josiphos ligands, *J. Org. Chem.* 74 (2009) 135–143, <https://doi.org/10.1021/jo801824e>.
- [44] A.A. Ibrahim, P.H. Wei, G.D. Harzmann, N.J. Kerrigan, Josiphos-catalyzed asymmetric homodimerization of ketoenones, *J. Org. Chem.* 75 (2010) 7901–7904, <https://doi.org/10.1021/jo101867m>.
- [45] S.K. Gibbons, R.P. Hughes, D.S. Glueck, A.T. Royappa, A.L. Rheingold, R.B. Arthur, A.D. Nicholas, H.H. Patterson, Synthesis, structure, and luminescence of copper(I) halide complexes of chiral bis(phosphines), *Inorg. Chem.* 56 (2017) 12809–12820, <https://doi.org/10.1021/acs.inorgchem.7b01562>.
- [46] S.U. Son, K.H. Park, Y.S. Lee, B.Y. Kim, C.H. Choi, M.S. Lan, Y.H. Jang, D.J. Jang, Y. K. Chung, Synthesis of Ru(II) complexes of N-heterocyclic carbenes and their promising photoluminescence properties in water, *Inorg. Chem.* 43 (2004) 6896–6898, <https://doi.org/10.1021/ic049514f>.
- [47] T.Y. Li, X. Liang, L. Zhou, C. Wu, S. Zhang, X. Liu, G.Z. Lu, L.S. Xue, Y.X. Zheng, J. L. Zuo, N-heterocyclic carbenes: versatile second cyclometalated ligands for neutral iridium(III) heteroleptic complexes, *Inorg. Chem.* 54 (2015) 161–173, <https://doi.org/10.1021/ic501949h>.
- [48] J. Vrána, J. Holub, Z. Ruiszicková, J. Janfrlík, D. Hnyk, A. Ruiszicka, Investigation of thiaborane closo-nido conversion pathways promoted by N-heterocyclic carbenes, *Inorg. Chem.* 58 (2019) 2471–2482, <https://doi.org/10.1021/acs.inorgchem.8b03037>.
- [49] F. Fantuzzi, C.B. Coutinho, R.R. Oliveira, M.A.C. Nascimento, Diboryne Nanostructures stabilized by multipot n-heterocyclic carbenes: a computational study, *Inorg. Chem.* 57 (2018) 3931–3940, <https://doi.org/10.1021/acs.inorgchem.8b00089>.
- [50] A. Kausamo, H.M. Tuononen, K.E. Krahulic, R. Roesler, N-heterocyclic carbenes with inorganic backbones: electronic structures and ligand properties, *Inorg. Chem.* 47 (2008) 1145–1154, <https://doi.org/10.1021/ic7020929>.
- [51] T.I. Kückmann, U. Abram, Rhenium(V) oxo complexes with N-heterocyclic carbenes, *Inorg. Chem.* 43 (2004) 7068–7074, <https://doi.org/10.1021/ic0497578>.
- [52] W.S. Mialki, R.E. Wild, R.A. Walton, Seven-coordinate alkyl isocyanide and mixed-alkyl isocyanide-phosphine complexes of tungsten(II), *Inorg. Chem.* 20 (1981) 1380–1384, <https://doi.org/10.1021/ic50219a010>.
- [53] D. Christendat, R.D. Markwell, D.F.R. Gilson, I.S. Butler, J.D. Cotton, Quadrupole-dipole effects in solid-state phosphorus-31 CP-MAS NMR spectra of tertiary phosphine substituted alkyl- and acyltetra-carbonylmanganese(I) complexes, *Inorg. Chem.* 36 (1997) 230–235, <https://doi.org/10.1021/ic960476c>.
- [54] R.B. King, J.A. Zinich, J.C. Cloyd, Poly (tertiary phosphines and arsines). XII. Some metal complexes of methylated di- and tri(tertiary phosphines), *Inorg. Chem.* 14 (1975) 1554–1559, <https://doi.org/10.1021/ic50149a022>.
- [55] X. Liu, N. Thirupathi, I.A. Guzei, J.G. Verkade, An investigation of staudinger reactions involving cis-1,3,5- triazidocyclohexane and tri(alkylamino)phosphines, *Inorg. Chem.* 43 (2004) 7431–7440, <https://doi.org/10.1021/ic0492845>.
- [56] N. Marion, S.P. Nolan, Well-defined N-heterocyclic carbenes-palladium(II) precatalysts for cross-coupling reactions, *Acc. Chem. Res.* 41 (2008) 1440–1449, <https://doi.org/10.1021/ar800020y>.
- [57] M.M. Heravi, Z. Kheilkordi, V. Zadsirjan, M. Heydari, M. Malmir, Buchwald-Hartwig reaction: an overview, *J. Organomet. Chem.* 861 (2018) 17–104, <https://doi.org/10.1016/j.jorganchem.2018.02.023>.
- [58] F. Rataboul, A. Zapf, R. Jackstell, S. Harkal, T. Riermeier, A. Monsees, U. Dingerdissen, M. Beller, New ligands for a general palladium-catalyzed amination of aryl and heteroaryl chlorides, *Chem. - A Eur. J.* 10 (2004) 2983–2990, <https://doi.org/10.1002/chem.200306026>.
- [59] Q. Dai, W. Gao, D. Liu, L.M. Kapes, X. Zhang, Triazole-based monophosphine ligands for palladium-catalyzed cross-coupling reactions of aryl chlorides, *J. Org. Chem.* 71 (2006) 3928–3934, <https://doi.org/10.1021/jo060321e>.
- [60] R.A. Singer, M. Doré, J.E. Sieser, M.A. Berliner, Development of nonproprietary phosphine ligands for the Pd-catalyzed amination reaction, *Tetrahedron Lett.* 47 (2006) 3727–3731, <https://doi.org/10.1016/j.tetlet.2006.03.132>.
- [61] C.A. Fleckenstein, H. Plenio, 9-Fluorenylphosphines for the Pd-catalyzed Sonogashira, Suzuki, and Buchwald-Hartwig coupling reactions in organic solvents and water, *Chem. - A Eur. J.* 13 (2007) 2701–2716, <https://doi.org/10.1002/chem.200601142>.
- [62] N. Schwarz, A. Tillack, K. Alex, I.A. Sayyed, R. Jackstell, M. Beller, A novel palladium catalyst for the amination of electron-rich indole derivatives, *Tetrahedron Lett.* 48 (2007) 2897–2900, <https://doi.org/10.1016/j.tetlet.2007.02.082>.
- [63] S. Doherty, J.G. Knight, C.H. Smyth, G.A. Jorgenson, Electron-rich, bicyclic biaryl-Like KITPHOS monophosphines via [4+2] cycloaddition between 1-alkynylphosphine oxides and anthracene: highly efficient ligands for palladium-catalyzed C–N and C–C bond formation, *Adv. Synth. Catal.* 350 (2008) 1801–1806, <https://doi.org/10.1002/adsc.200800307>.
- [64] C.M. So, Z. Zhou, C.P. Lau, F.Y. Kwong, Palladium-catalyzed amination of aryl mesylates, *Angew. Chemie - Int. Ed.* 47 (2008) 6402–6406, <https://doi.org/10.1002/anie.200802157>.
- [65] K. Suzuki, Y. Hori, T. Kobayashi, A new hybrid phosphine ligand for palladium-catalyzed amination of aryl halides, *Adv. Synth. Catal.* 350 (2008) 652–656, <https://doi.org/10.1002/adsc.200700543>.
- [66] G.J. Withbroe, R.A. Singer, J.E. Sieser, Streamlined synthesis of the bippypfos family of ligands and cross-coupling applications, *Org. Process Res. Dev.* 12 (2008) 480–489, <https://doi.org/10.1021/op7002858>.
- [67] M.M. Heravi, N. Nazari, Bischler-Napieralski reaction in total synthesis of isoquinoline-based natural products. An old reaction, a new application, *Curr. Org. Chem.* 19 (2015) 2358–2408, <https://doi.org/10.2174/1385272819666150730214506>.
- [68] R. Pratap, D. Parrish, P. Gunda, D. Venkataraman, M.K. Lakshman, Influence of biaryl phosphine structure on C-N and C-C bond formation, *J. Am. Chem. Soc.* 131 (2009) 12240–12249, <https://doi.org/10.1021/ja902679b>.
- [69] J. Ruan, L. Shearer, J. Mo, J. Bacsa, A. Zanotti-Gerosa, F. Hancock, X. Wu, J. Xiao, Paracyclophane-based monophosphine ligand for palladium-catalyzed cross-coupling reactions of aryl chlorides, *Org. Biomol. Chem.* 7 (2009) 3236–3242, <https://doi.org/10.1039/b906139h>.
- [70] K. Suzuki, Y. Hori, T. Nishikawa, T. Kobayashi, A. Novel, (2,2-Diarylvinylyl) phosphine/Palladium catalyst for effective aromatic amination, *Adv. Synth. Catal.* 349 (2007) 2089–2091, <https://doi.org/10.1002/adsc.2007000220>.
- [71] B. Punji, J.T. Mague, M.S. Balakrishna, Synthesis of neutral (PdII, PtII), cationic (Pd II), and water-induced anionic (PdII) complexes containing new mesocyclic thioether-aminophosphonite ligands and their application in the Suzuki cross-coupling reaction, *Inorg. Chem.* 45 (2006) 9454–9464, <https://doi.org/10.1021/ic061419e>.
- [72] B. Punji, J.T. Mague, M.S. Balakrishna, Thioether-functionalized ferrocenyl-bis (phosphonite), $\text{Fe}(\text{C} 5\text{H}_4\text{P}(\text{O} \text{C} 10\text{H}_6(\mu\text{-S} \text{C} 10\text{H}_6\text{O}))_2)$: synthesis, coordination behavior, and application in Suzuki-Miyaura cross-coupling reactions, *Inorg. Chem.* 46 (2007) 10268–10275, <https://doi.org/10.1021/ic701537k>.
- [73] B. Karimi, P. Fadavi Akhavan, A study on applications of N-substituted main-chain NHC-palladium polymers as recyclable self-supported catalysts for the Suzuki-Miyaura coupling of aryl chlorides in water, *Inorg. Chem.* 50 (2011) 6063–6072, <https://doi.org/10.1021/ic2000766>.
- [74] K.V. Vivekananda, S. Dey, D.K. Maity, N. Bhuvanesh, V.K. Jain, Supramolecular macrocyclic Pd(II) and Pt(II) squares and rectangles with arylidithiolate ligands and their excellent catalytic activity in Suzuki C-C coupling reaction, *Inorg. Chem.* 54 (2015) 10153–10162, <https://doi.org/10.1021/acs.inorgchem.5b00806>.
- [75] L.M. Zhang, H.Y. Li, H.X. Li, D.J. Young, Y. Wang, J.P. Lang, Palladium(II) chloride complexes of N,N'-disubstituted imidazole-2-thiones: syntheses, structures, and catalytic performances in Suzuki-Miyaura and sonogashira coupling reactions,

- Inorg. Chem. 56 (2017) 11230–11243, <https://doi.org/10.1021/acs.inorgchem.7b01616>.
- [76] A.V. Vorogushin, X. Huang, S.L. Buchwald, Use of tunable ligands allows for intermolecular Pd-catalyzed C-O bond formation, *J. Am. Chem. Soc.* 127 (2005) 8146–8149, <https://doi.org/10.1021/ja050471r>.
- [77] S.A. Dandekar, S.N. Greenwood, T.D. Greenwood, S. Mabic, J.S. Merola, J. M. Tanko, J.F. Wolfe, Synthesis of succinimido[3,4-b]indane and 1,2,3,4,5,6-hexahydro-1,5-methano-3-benzazocine-2,4-dione by sequential alkylation and intramolecular arylation of enolates derived from N,N,N',N'-tetramethylbutanediamides and N,N,N',N'-tetramethylpentanediamides, *J. Org. Chem.* 64 (1999) 1543–1553, <https://doi.org/10.1021/jo982000b>.
- [78] S. Teyrulnikov, M.C. Kozlowski, Accounting for strong ligand sensitivity in Pd-catalyzed α -arylation of enolates from ketones, esters, and nitroalkanes, *J. Org. Chem.* 85 (2020) 3465–3472, <https://doi.org/10.1021/acs.joc.9b03203>.
- [79] M.C. Willis, D. Taylor, A.T. Gillmore, Palladium-catalyzed intramolecular O-arylation of enolates: application to benzo[6]furan synthesis, *Org. Lett.* 6 (2004) 4755–4757, <https://doi.org/10.1021/ol047993g>.
- [80] Z.F. Xu, C.X. Cai, M. Jiang, J.T. Liu, Copper-catalyzed regio- and stereoselective O-arylation of enolates, *Org. Lett.* 16 (2014) 3436–3439, <https://doi.org/10.1021/ol501434d>.
- [81] C.H. Burgos, T.E. Barder, X. Huang, S.L. Buchwald, Significantly improved method for the Pd-catalyzed coupling of phenols with aryl halides: understanding ligand effects, *Angew. Chemie - Int. Ed.* 45 (2006) 4321–4326, <https://doi.org/10.1002/anie.200601253>.
- [82] G.L. A. Najibi, The nonlocal kernel in van der waals density functionals as an additive correction: an extensive analysis with special emphasis on the B97M-V and ω B97M-V approaches, *J. Chem. Theory Comput.* 11 (2018) 5725–5738.
- [83] F.W. R. Ahlrichs, No Title, *Phys. Chem.* 7 (2005) 3297.
- [84] P. Comba, A. Merbach, The titanyl question revisited, *Inorg. Chem.* 26 (1987) 1315–1323, <https://doi.org/10.1021/ic00255a024>.
- [85] B.C. Satyendra N. Shukla, Pratiksha Gaur, Dimple Dehariya, Schiff base complexes of titanocene dichloride: synthesis, characterization, dft modeling, Antibacterial and catalytic activity, *Int. J. Basic Appl. Chem. Sci.* 9 (2019) 1–20.
- [86] M.S. Oderinde, N.H. Jones, A. Juneau, M. Frenette, B. Aquila, S. Tentarelli, D. W. Robbins, J.W. Johannes, Highly chemoselective iridium photoredox and nickel catalysis for the cross-coupling of primary aryl amines with aryl halides, *Angew. Chemie.* 128 (2016) 13413–13417, <https://doi.org/10.1002/ange.201604429>.
- [87] E.B. Corcoran, M.T. Pirnot, S. Lin, S.D. Dreher, D.A. DiRocco, I.W. Davies, S. L. Buchwald, D.W.C. Macmillan, Aryl amination using ligand-free Ni(II) salts and photoredox catalysis, *Science (80-)* 353 (2016) 279–283, <https://doi.org/10.1126/science.aag0209>.
- [88] J.B. Diccianni, T. Diao, Mechanisms of nickel-catalyzed cross-coupling reactions, *Trends Analyt. Chem.* 1 (2019) 830–844, <https://doi.org/10.1016/j.trechm.2019.08.004>.